DSTO

New Techniques to Predict Ship Vulnerability to Pressure Mines along Shipping Routes

John C. Barnes

DSTO-RR-0126

DEPARTMENT ◆ OF DEFENCE

DEFENCE SCIENCE AND TECHNOLOGY ORGANISATION

New Techniques to Predict Ship Vulnerability to Pressure Mines along Shipping Routes

John C. Barnes

Maritime Operations Division
Aeronautical and Maritime Research Laboratory

DSTO-RR-0126

ABSTRACT

New techniques have been developed which allow for real time prediction of ship vulnerability to pressure mines at all points along the shipping routes approaching and within Australia's priority ports. Rather than performing an extensive series of measurements, environmental bottom pressure fluctuations can be predicted using data from existing offshore wave measuring systems. The techniques have been validated by measurements in Sydney Harbour. In addition, sweep effectiveness can be predicted in real time, and seasonal averages of ship vulnerability and sweep effectiveness calculated for planning purposes.

RELEASE LIMITATION

Approved for public release

DEPARTMENT OF DEFENCE

DEFENCE SCIENCE AND TECHNOLOGY ORGANISATION

Published by

DSTO Aeronautical and Maritime Research Laboratory
PO Box 4331
Melbourne Victoria 3001 Australia

Telephone: (03) 9626 7000
Fax: (03) 9626 7999

AR-010-458
February 1998

APPROVED FOR PUBLIC RELEASE

New Techniques to Predict Ship Vulnerability to Pressure Mines along Shipping Routes

Executive Summary

Naval pressure mines are designed to detect the reduction in pressure at the sea bottom as a ship passes overhead. This pressure signal must be detected in the presence of environmental bottom pressure fluctuations caused by the local wave conditions, which vary in amplitude by orders of magnitude with time and place. Consequently, ship vulnerability to pressure mines is strongly dependent on the local wave environment.

Current methods to predict ship vulnerability require the input of the environmental bottom pressure spectra for the site of interest. Real time evaluation of ship vulnerability at all points along a shipping route is impractical using these methods because of the multitude of bottom pressure measurements required. This report describes the validation of new methods implemented in the Total Mine Simulation System (TMSS) to predict bottom pressure spectra along shipping routes from existing offshore wave measuring systems.

Surface wave spectra were obtained from a directional Waverider buoy located off Sydney Harbour. Refraction modelling of waves entering Sydney Harbour was used to predict the attenuation of the various spectral components as they move inshore. Linear wave theory was used to predict the bottom pressure spectra from the surface wave spectra. Measurements of actual bottom spectra were made on 4 separate occasions at 3 or 4 sites. Comparison with predictions showed excellent agreement in amplitude, and reasonable agreement in zero crossing period and spectral width. Predictions of mine actuation probability using the predicted and measured spectra agreed closely, which is the fundamental test of the technique.

Mine sweeping is a mine neutralization process aimed at actuating mines in the absence of target ships by producing similar magnetic, acoustic and other fields. Pressure mines generally incorporate acoustic and/ or magnetic sensors together with the pressure sensor, and so pressure minesweeping generally involves towing of an acoustic or magnetic field generator while relying on the background swell to produce the required suction at the required time. Pressure sweep effectiveness as a function of position is easily calculated using the new techniques, aiding decisions regarding the allocation of minesweeping and other mine countermeasure resources. Seasonal averages of ship vulnerability and sweep effectiveness can also be calculated which are more useful for long term planning than measurements at one particular time.

A detailed analysis of the uncertainties in the prediction techniques has suggested various improvements. However, given the success of the existing techniques, the main priority for future work is to apply the techniques to northern priority ports where minelaying is more likely.

Author

John C. Barnes
Maritime Operations Division

John C. Barnes has a PhD in Physics from the University of Sydney. Joining DSTO in 1991, he was initially employed in operations research before switching to mine warfare in 1993. In 1994 he assumed responsibility for pressure mine countermeasures research, which aims to enable the prediction of the vulnerability of a ship to a given pressure mine at specified locations, together with the probability of sweeping the mine using the background swell. The work encompasses the measurement and analysis of ship pressure signatures and pressure fluctuations due to surface waves together with research into mine technology. After spending a workday studying the wave environment along shipping routes, John enjoys returning to his beachhouse and riding God's waves on his windsurfer.

Contents

1. Introduction

A naval mine is an explosive device designed to actuate after placement if a target ship comes in contact or passes nearby. Pressure sensors in naval ground mines (located on the sea bottom) are designed to detect the reduction in pressure which occurs below a ship. Wind waves, swell and tides also cause fluctuations in bottom pressure, which the mine must try to distinguish from the ship signature. The threat to shipping from pressure mines is strongly dependent on the environmental bottom pressure fluctuations caused by the ambient sea conditions. Consequently, a knowledge of the background pressure environment is required for all points along the shipping routes approaching and within Australia's priority ports.

The pressure reduction generated by a ship has magnitude of order 100 mm head of water (1000 Pa), and is sustained for a time interval comparable to the time taken for the length of the ship to transit past the mine (typically greater than 10 seconds) [2]. Tides are easily distinguished from the ship signature because of their long period. Pressure fluctuations from wind waves with period less than a few seconds are strongly attenuated with depth, and so are not usually a problem for the mine designer. Most swell wave energy at locations around Australia is concentrated between periods of 7 and 20 seconds [6, Appendix 4]. Depending on the sophistication of the mine, short period swell may be reduced by filtering. Longer period swell can not be removed because of the frequency overlap with the ship signal. Generally pressure mines also require appropriate acoustic and magnetic fields for actuation, and so can not be actuated by background swell alone.

Minesweeping is the process of neutralising a mine threat by tricking the mines into detonating in the absence of a target ship. Typically, acoustic and magnetic mines are swept by towing an acoustic or magnetic source through the minefield. Pressure minesweeping generally involves towing of an acoustic or magnetic field generator while relying on the background swell to produce the required suction at the required time. Pressure sweep effectiveness is highly dependent on the background wave environment.

Bottom pressure fluctuations vary in size by orders of magnitude with time and location, depending on the weather and the protection from offshore swell. In offshore locations, pressure mines frequently pose minimal threat because of large environmental bottom pressure fluctuations, while at sheltered locations, the threat is high. Ideally a system is required, whereby given a mine and its settings, the mine actuation probability for a given ship or sweep can be displayed on a chart of a priority port, showing the probability averaged over the year or season, or the current probability. This would then allow the subdivision of shipping routes into regions where pressure mines were not a threat, regions where pressure mines could be swept and regions where mine hunting (using sonar to find the mines) would be required. Figure 1 is an example of the type of information required and aimed for as part of Task ADS 93/230, "Acoustic and Pressure Mine Countermeasures".

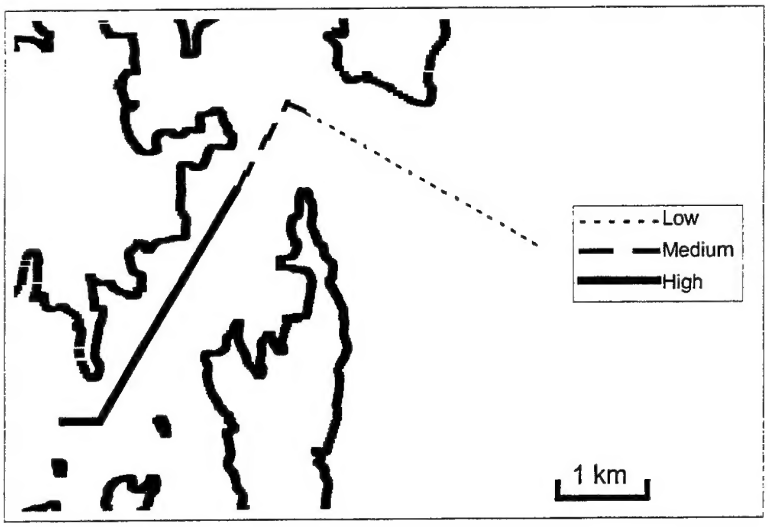

Figure 1. Example of Required Display of Ship Vulnerability to Pressure Mines for Sydney Harbour Shipping Route
Display is for a particular target type and speed, and mine type and setting. Details are classified.

Currently, the Total Mine Simulation System (TMSS) computer model [5] can be used to predict the threat from a given pressure mine to a given target at a given time and place, assuming that the spectrum of the bottom pressure variations is known. For real time use, it is impractical to make measurements of the spectra at all points along the shipping routes. Indeed, the RAN mine warfare forces do not possess even one of the multitude of bottom pressure sensors required for this approach. Instead, the approach tested in this report is to use measurements of offshore conditions, (made with existing installations), to predict the bottom pressure environment at all inshore locations along the shipping routes.

2. Method

2.1 Prediction of Bottom Pressure Fluctuations from the Offshore Waverider

Offshore wave conditions are monitored in real time at many Australian ports [6]. In many cases, several years of records are available, allowing accurate annual or seasonal averages to be calculated. In this experiment, data from the Manly Hydraulics Laboratory Sydney Directional Waverider Buoy was used [11]. Waverider buoys float on the sea surface, monitoring changes in the position of the sea surface with one or more accelerometers. This information is then radioed to a shore station for analysis. Manly Hydraulics Laboratory supplied directional spectral files, which give the spectral energy density and mean direction for 64 frequency bins. These range from

0.025 Hz (corresponding to a 40 second period) to 0.58 Hz (corresponding to a 1.7 second period), although the accuracy of the Waverider buoy is poor for frequencies less than 0.05 Hz [10, p18; 14]. The data is based on measurements of 256 waves (giving a typical record length of 15 to 35 minutes). An example of the data from the directional Waverider is shown in Figure 2.

Wave refraction modelling for Sydney Harbour was performed under contract by Lawson and Treloar Pty Ltd (Appendix 1). Predictions of attenuation coefficients, (defined as the ratio of the inshore to offshore wave height) for offshore wave spectral components of seven frequencies and six directions were made for 47 sites along the shipping routes in Sydney Harbour (Fig. 3). An example of the attenuation coefficients for one site is shown in Figure 4. Lower frequencies were emphasised in the modelling, because these are characteristic of ship signatures [2], while waves from the SE quadrant were emphasised due to the predominance of swell from this direction [7]. Linear interpolation was used to calculate the attenuation coefficients for all the various frequencies and directions of the offshore wave components.

Bottom pressure spectra were calculated from the surface wave spectra at each site using linear wave theory [13]. High frequency waves are strongly attenuated, while lower frequencies are only slightly attenuated.

Figure 5 shows the various stages of the analysis outlined above; namely, the offshore surface wave spectrum at a given time, the predicted surface wave spectrum at site 20 and the predicted bottom pressure spectrum at the same site.

Having calculated the bottom pressure spectrum at the site of interest, the full capability of the TMSS computer model can be used to predict the mine actuation probability for various combinations of target type, speed and abeam distance and mine type and setting. This requires multiple simulated engagements for each scenario in which the pressure changes at the mine caused by the combination of ship passage and background environmental fluctuations are calculated to determine the probability of mine actuation. The current spectrum can be used to calculate the current actuation probability, or a selection of historical spectra used to predict seasonal averages for planning purposes.

Frequency (Hz)	Spectral Density (mm^2/Hz)	Direction (deg)
0.025	1010	260
0.030	1185	253
0.035	779	119
0.040	1850	10
0.045	2691	119
0.050	5529	93
0.055	19394	133
0.060	74810	136
0.065	43814	124
0.070	269064	150
0.075	93686	133
0.080	468693	155
0.085	862598	166
0.090	713333	148
0.095	632670	159
0.100	953318	156
0.110	578217	153
0.120	709776	148
0.130	1199846	148
0.140	862598	145
0.150	520583	132
0.160	340341	142
0.170	235085	140
0.180	177674	133
0.190	175028	148
0.200	154462	139
0.210	67353	132
0.220	42732	136
0.230	34293	135
0.240	30568	129
0.250	23452	133
0.260	40043	148
0.270	37149	121
0.280	24778	124
0.290	27384	107
0.300	21114	121
0.310	27111	91
0.320	22197	107
0.330	18083	131
0.340	19010	129
0.350	21114	104
0.360	13065	174
0.370	14367	126
0.380	6924	119
0.390	8542	110
0.400	10381	167
0.410	9025	145
0.420	7315	38
0.430	7846	313
0.440	7389	166
0.450	6172	173
0.460	4035	167
0.470	5285	149
0.480	5900	193
0.490	4526	32
0.500	4595	315
0.510	5841	181
0.520	4242	90
0.530	3579	66
0.540	2085	90
0.550	3049	131
0.560	2459	157
0.570	2085	93
0.580	2203	87

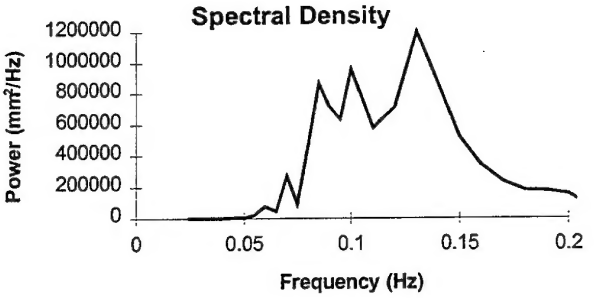

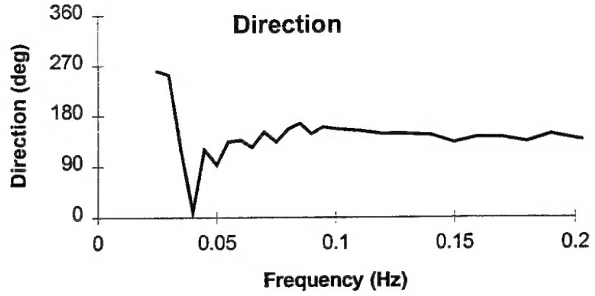

Figure 2. Example of Data from the Directional Waverider

The data from the Sydney directional Waverider buoy at 10 am on 26th October 1995 is shown. Other parameters also provided include the significant wave height of 1.1m and the mean zero crossing period of 6.6 seconds.

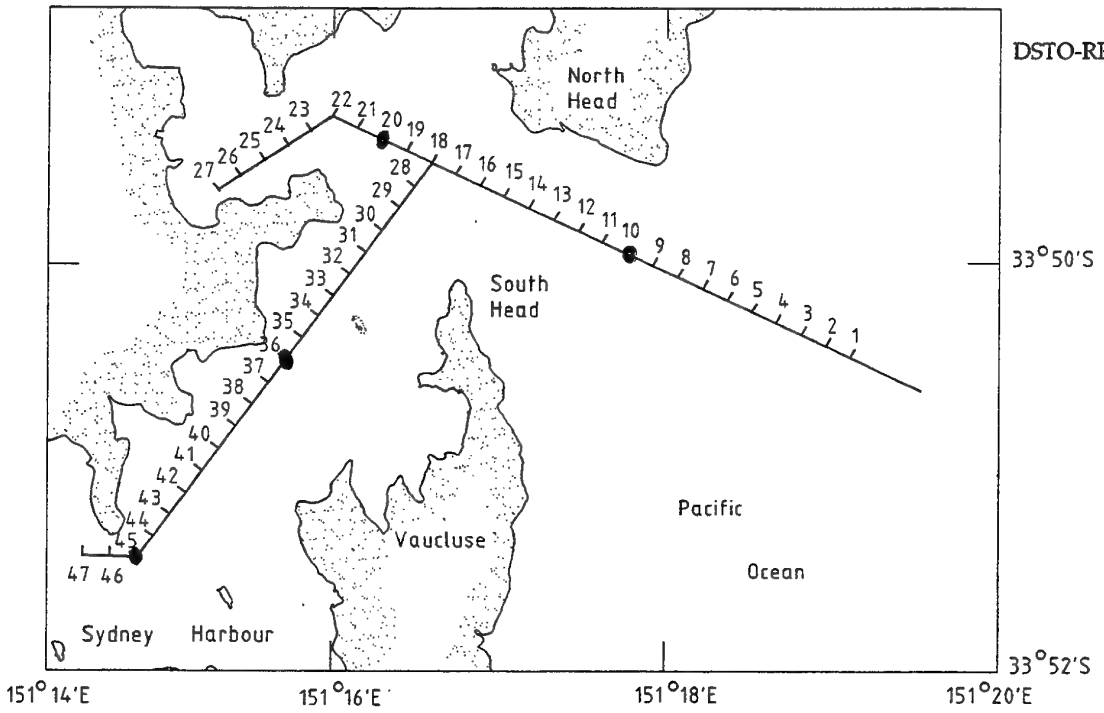

Figure 3. Sites for Computed Attenuation Data
Field measurement sites shown thus ●

Frequency (Hz)	Direction (deg)					
	45	90	112.5	135	157.5	180
0.02	0.56	0.52	0.90	1.04	0.72	0.30
0.05	0.26	0.59	0.80	0.73	0.52	0.31
0.07	0.25	0.56	0.75	0.68	0.48	0.28
0.08	0.23	0.52	0.70	0.62	0.43	0.26
0.10	0.20	0.49	0.67	0.58	0.39	0.23
0.13	0.16	0.45	0.68	0.57	0.36	0.18
0.20	0.08	0.38	0.89	0.72	0.35	0.11

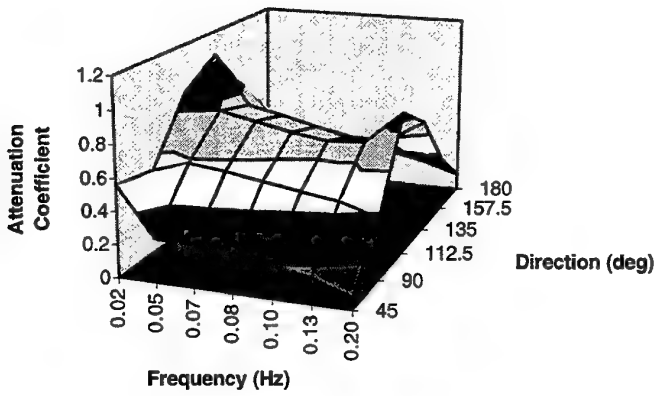

Figure 4. Example of Attenuation Coefficients for One Site (Site 20)
The axes on the plot are non-linear because the data is concentrated at lower frequencies and directions from the SE quadrant.

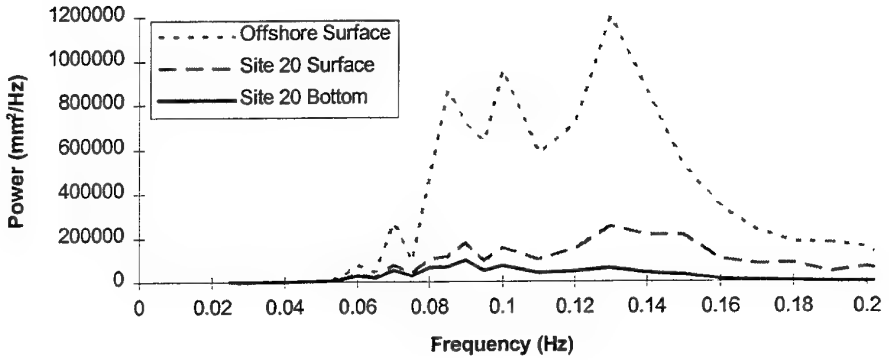

Figure 5. Prediction of Bottom Pressure Spectrum from Offshore Surface Wave Spectrum Offshore surface wave spectrum from 10 am, 26 October 1995 (Fig. 2) used, together with attenuation coefficients for Site 20 shown in Figure 4.

Currently, the calculations must be repeated for the various points along the shipping routes to obtain presentations such as shown in Figure 1. Although this simply involves changing the site and depth for each simulation, automation of this process is envisaged in the long term.

Full details of the implementation of the above procedures have been documented [3], and are available from the author on request. Most TMSS modifications were designed to handle the offshore swell direction and site attenuation data. In addition, some general improvements have also been made to the TMSS swell generation routines. First, program speed has been greatly increased by calculating the attenuation of the spectral components with depth in the initialization routine for each engagement, rather than at each time step in the simulated engagement. Secondly, increased flexibility has been added to the process of generating the wave record, which is performed by the linear superposition of the various frequency components in the spectrum i.e. $\sum A_i \sin(f_i(t + t_{offset}) + 2\pi\phi_i))$. Previously, for each simulated engagement, the wave enviroment was randomized by varying the time offset t_{offset}, while the phase ϕ_i of the components was fixed. However for frequencies f_i = 1/1024, 2/1024, ..., 512/1024 the simulated swell repeats after 1024 seconds, limiting the number of independent simulated engagements. For example, a swell file starting at 100 seconds is the same as one starting at 1124 seconds. To avoid this problem, the option of randomly generating the phase ϕ_i of each spectral component for each engagement has been added.

2.2 Measurements of Bottom Pressure Fluctuations

Bottom pressure measurements were made on 4 separate days at 3 or 4 harbour locations, near sites 10, 20, 36, and 45 (Fig. 3). A Seapac 2200 Wave and Tide Gauge

(Woods Hole Instrument Systems Ltd) was used for about 40 minutes at each site, sampling at 2 Hz.

For each measurement, spectra were calculated from a 34 minute section of the record using a wave analysis program developed by Saiva [12]. Before performing the fast fourier transform in the program, the linear trend was removed from each of the two consecutive 2048 point segments to reduce the strong low frequency tidal component. Spectral energy density estimates were averaged over the two segments and band averaged over seven frequencies. No windowing was used.

The measured bottom pressure spectra were used in TMSS to calculate mine actuation probabilities.

2.3 Comparison of Predictions and Measurements

Verification of the techniques involved comparison of the predicted and measured spectra of the bottom pressure fluctuations, particularly the mean amplitude, zero crossing period and spectral width. Predictions of actuation probability made using the offshore Waverider data were also compared with calculations of actuation probability made using the measured bottom pressure data. This was done for a few different combinations of target type, speed and abeam distance and mine type and setting.

3. Results

3.1 Spectra

A rigorous test of the techniques outlined in this report is to compare the measured and predicted bottom spectra. Agreement would strongly suggest that the predicted and measured actuation probabilities would agree for all target and mine combinations. Any systematic errors in the theory are also likely to be apparent.

Figure 6 illustrates the comparison between the measured and predicted pressure spectra. There is general agreement in the overall magnitude and the dominant frequencies.

Firstly, Figure 6 shows that the overall magnitude of the predicted and measured spectra agree quite closely, given that the magnitude typically varies by more than an order of magnitude between the various sites on any given day. Figure 7(a) confirms this, showing the agreement between the predicted and measured mean amplitude. The predictions equal the measurements with correlation coefficient $r^2 = 0.96$.

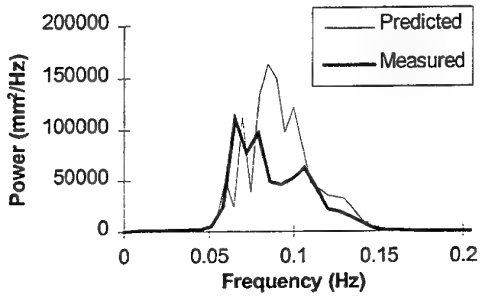

(a) 26 Oct Site 10

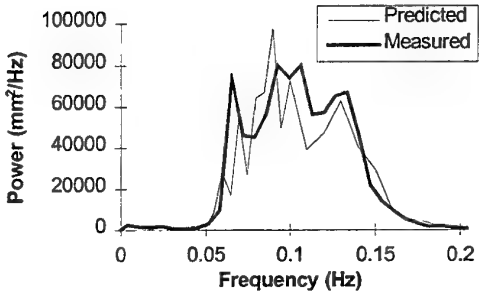

(b) 26 Oct Site 20

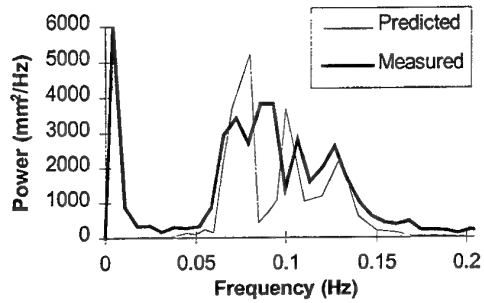

(c) 26 Oct Site 36

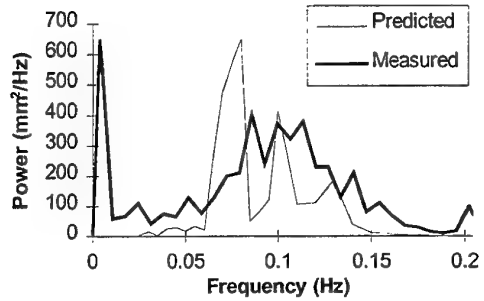

(d) 26 Oct Site 45

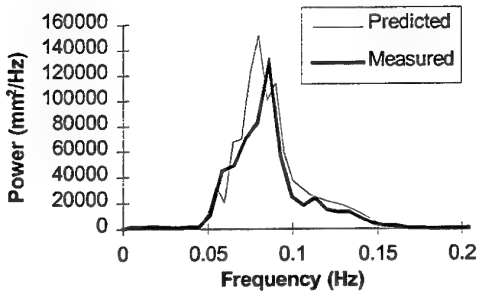

(e) 13 Sep Site 10

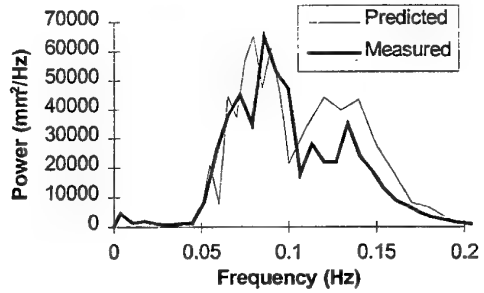

(f) 13 Sep Site 20

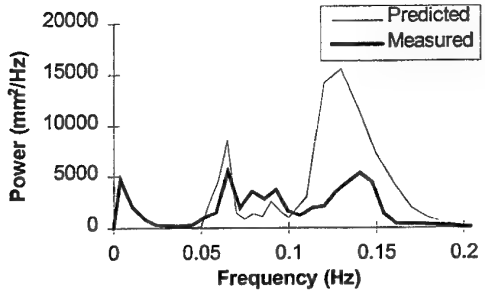

(g) 13 Sep Site 36

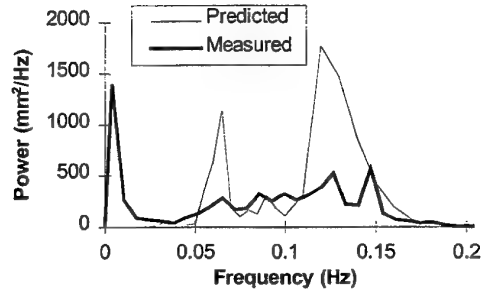

(h) 13 Sep Site 45

Figure 6. Comparison between Measured and Predicted Spectra (continued overleaf)

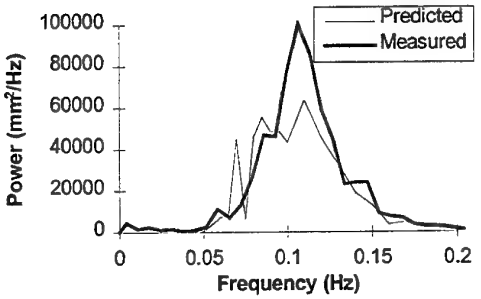

Not measured
(i) 4 July Site 10

(j) 4 July Site 20

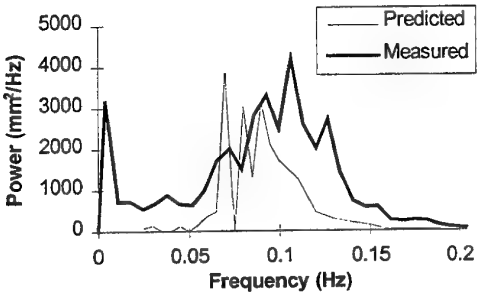

(k) 4 July Site 36

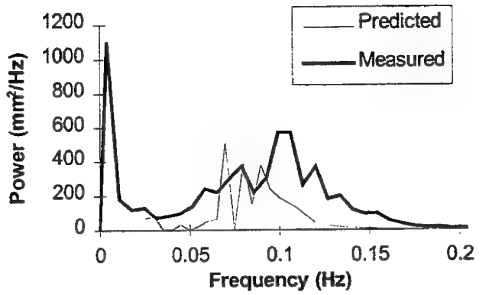

(l) 4 July Site 45

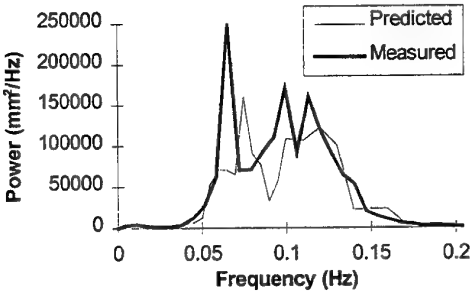

Not measured
(m) 6 June Site 10

(n) 6 June Site 20

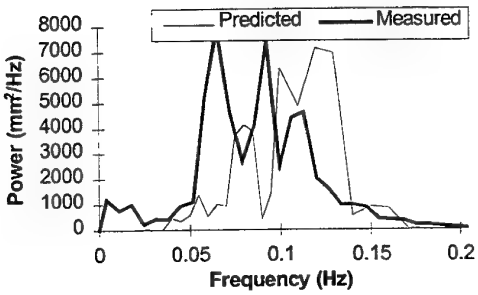

(o) 6 June Site 36

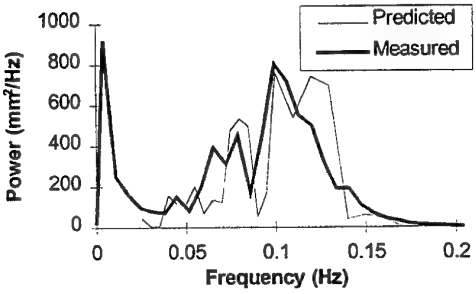

(p) 6 June Site 45

Figure 6 (cont.) Comparison between Measured and Predicted Spectra

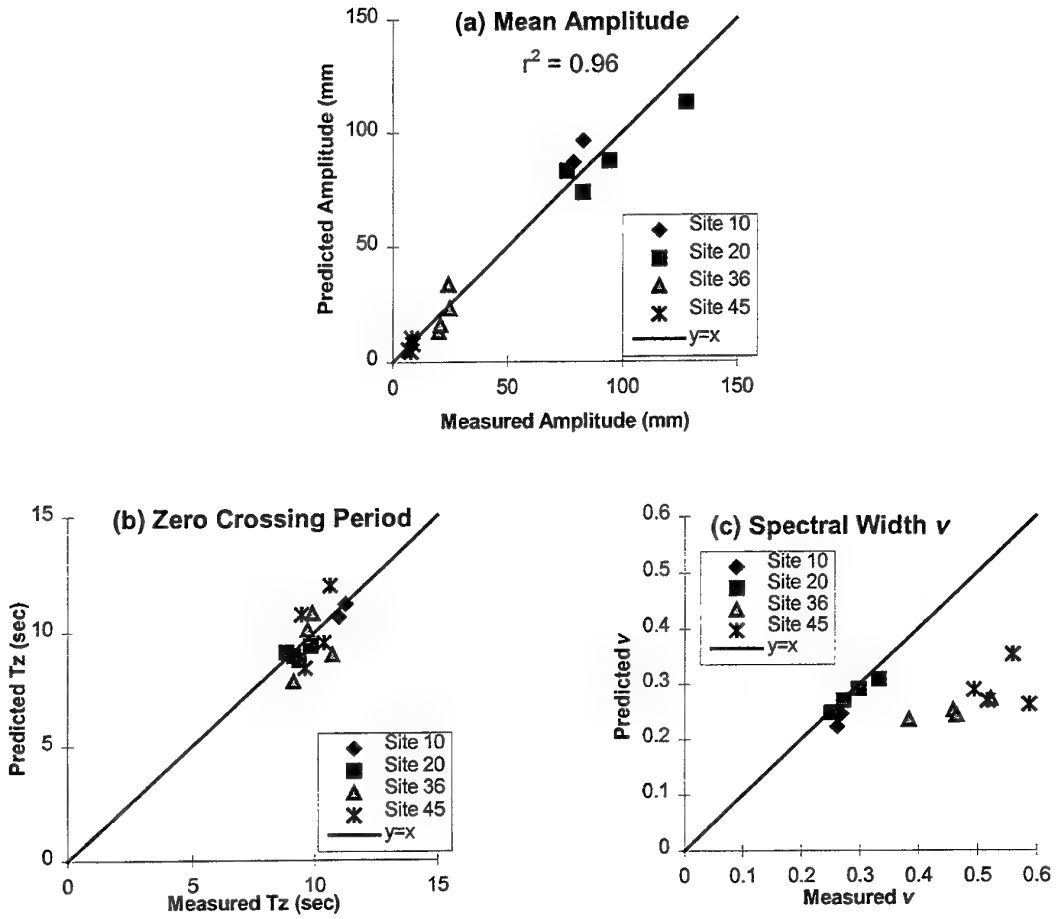

Figure 7. Comparison of Measured and Predicted Mean Amplitude, Zero Crossing Period and Spectral Width
As time series records are not available from the offshore predictions, all parameters have been estimated from the spectra as outlined in Reference 12.

Secondly, there is general agreement between the dominant frequencies of the predicted and measured spectra. One example of this is the agreement in the predicted and measured zero crossing period Tz shown in Figure 7(b), with the rms difference equal to 0.9 seconds. This is reasonable compared to the standard deviation of order 0.3 seconds obtained by directly measuring the bottom pressure fluctuations (Appendix 2).

Previous research at DSTO has established that the mine actuation probability is mainly affected by the mean amplitude and zero crossing period, but is also influenced by the spectral width in a complex manner [1]. For example, given Tz equals 10 seconds, and a mine requiring a pressure reduction to be sustained for 7 seconds, then an increase in spectral width may increase the wave energy with period greater than 14 seconds necessary to actuate the mine, but may also increase the

energy at lower frequencies, increasing the 'ripple' in the wave and thereby reducing the probability of the suction being maintained for the required time. Figure 7(c) shows less agreement in the spectral width parameter than in the other two with rms error of 35%. By comparison, the standard deviation in the spectral width obtained from bottom pressure measurements is of order 13% (Appendix 2). The agreement is worse for the calmer sites further into the harbour.

Estimates of the measured and predicted spectra are unlikely to agree exactly for several reasons. Besides the inherent uncertainty in estimating the spectrum from the finite length of the pressure record, there are uncertainties in each stage of predicting the bottom spectrum from the offshore wave record, which are discussed more fully in Appendix 2.

Most of the energy in the bottom spectra is concentrated in the frequency range 0.05 to 0.2 Hz, and at these frequencies uncertainties in the spectral estimates from the Waverider buoy and the bottom pressure measurements are significant uncertainties which each explain a large part of the differences between measurements and predictions.

At low frequencies, uncertainties in the directional estimates and errors in the directional modelling produce uncertainties equal to an order of magnitude. While the energy at these frequencies is less than in the main frequency range discussed above, pressure mines may be designed to focus on these frequencies because of the ship signature energy at these frequencies. Better modelling techniques should reduce these errors.

Waves generated by ferries and other small craft produce a small amount of background energy. This is significant for sheltered locations at the higher frequencies, but is likely to be less significant at other ports with less shipping.

The main systematic error between the predicted and measured spectra is caused by background shipping. Other systematic errors are the absence of very low frequencies in the Waverider predictions and some errors caused by the directional uncertainty at low frequencies. The combined effect of these systematic errors has little effect on the prediction of the mean amplitude and zero crossing period, but does lead to a systematic underprediction of the spectral width. Nevertheless, the method seems appropriate to extend to other harbours, particularly with the simple improvements suggested in Appendix 2.

Many ports around Australia are only served by non-directional Waveriders rather than the more modern and sophisticated directional version. The wave spectrum from the non-directional installations may be augmented by visual observation of the dominant swell direction (as opposed to measurement of the direction of all spectral components). Appendix 2 shows that the accuracy of the predictions is moderately degraded.

3.2 Actuation Probability

Ultimately, the real test of the effectiveness of the techniques presented in this report is the ability to accurately predict ship vulnerability or mine sweep effectiveness. This will generally be a less stringent test than the prediction of spectra because the actuation probability is primarily a function of a weighted average of the spectral components, and so accurate predictions of actuation probability can be made despite large random errors in the individual spectral components. For example, the actuation probability of a mine may be affected primarily by the total energy in the band 0.1 to 0.12 Hz, rather than the values of the individual components.

Figure 8 shows that the mine actuation probability predicted from the offshore directional Waverider agrees well with that obtained from measurements with the SP2200 pressure sensor. Combining all the results shown, the predicted mine actuation probability equals the measured mine actuation probability with correlation coefficient 0.96.

The actuation probability depends strongly on the mine type and setting. For example, an acoustic sweep may satisfy the acoustic requirements of a simple combination acoustic/pressure mine for a longer period than a more complex mine, increasing the time of the pressure look. Doubling of this time may double the sweep actuation probability. For the simple pressure mine the probability of actuation by swell will generally increase moving offshore, as shown in Figure 8 for the sweep, but for more sophisticated mines the suction threshold may increase, causing the actuation probability to decrease. The results in Figure 8 should not be interpreted as showing that the sweep actuation probability for pressure mines is always low, or that the actuation probability against merchant vessel targets is always high.

4. Conclusion

Estimates of environmental bottom pressure spectra along the main shipping route into Sydney Harbour agree closely with measurements, particularly in terms of mean amplitude. Predictions of pressure mine actuation probability also agree closely with measurements. While further research will improve the techniques, the main DSTO priority in this field is to obtain appropriate wave attenuation data to allow the techniques to be used for other priority Australian ports, particularly in northern Australia. Full details of the implementation of the above procedures have been documented [3], and are available from the author on request.

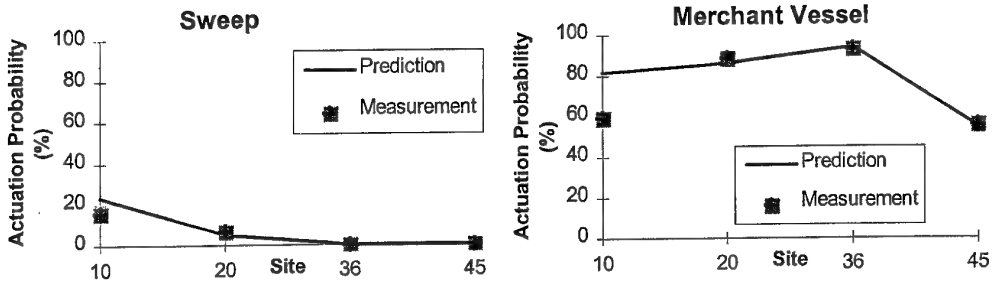

(a) October 26

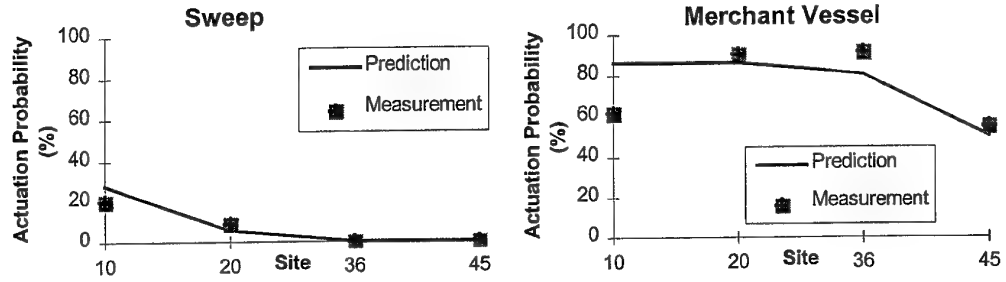

(b) September 13

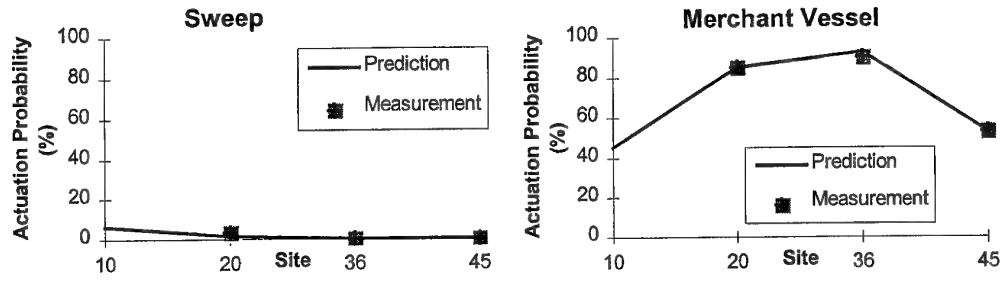

(c) July 4

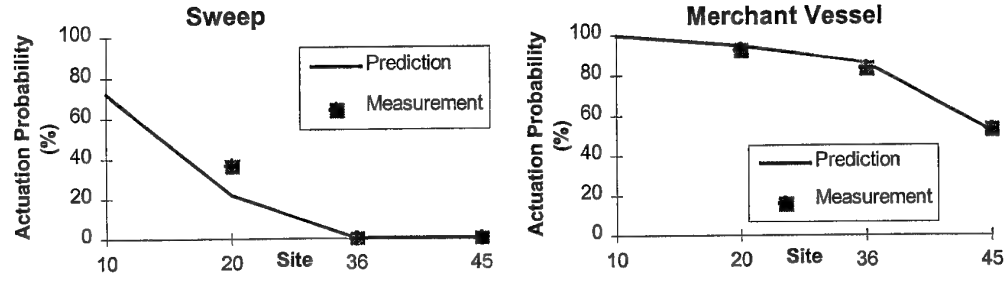

(d) June 6

Figure 8. Comparison of Actuation Probability Predicted from the Offshore Directional Waverider and Measured with the SP2200 Pressure Sensor

5. Acknowledgments

Mr Angus MacInnes skippered the DSTO workboat used to deploy the pressure sensor, catching a few fish in the process (picture). Mr Mark Kulmar provided data from the Manly Hydraulics Laboratory Directional Waverider Buoy, and was a friendly source of advice. Dr Doug Treloar of Lawson and Treloar Pty Ltd produced the wave refraction model as well as being a useful source of information.

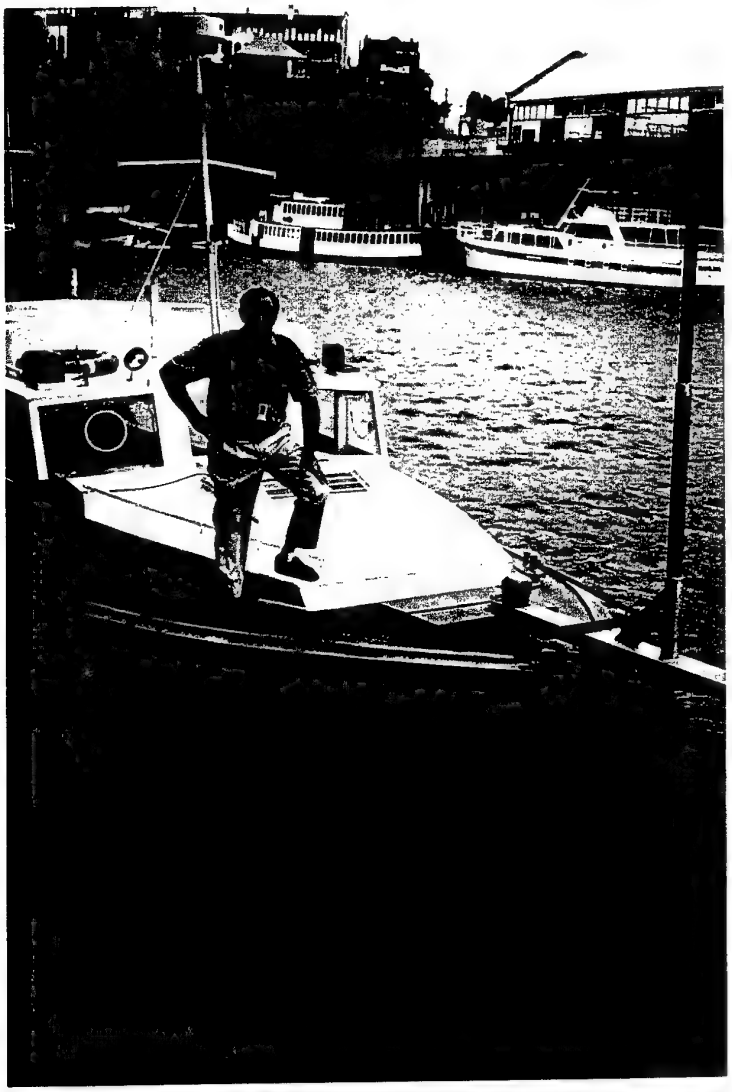

6. References

1. Barnes, John C., *Ambient Pressure Variations at the Sea Bed in Sydney Harbour and their Effect on Simple Pressure Mines*, DSTO Technical Report DSTO-TR-0154, (1995). CONFIDENTIAL

2. Barnes, John C., *Ship Pressure Signature Measurements*, DSTO Technical Report DSTO-TR-0250, (1996). CONFIDENTIAL

3. Barnes, John C., *Implementation in TMSS of New Techniques to Predict Ship Vulnerability to Pressure Mines along Shipping Routes*, DSTO Sydney Registry File 390-5-68(80), (22 February 1996).

4. Bishop, C.T. and Donelan, M.A., *Measuring Waves with Pressure Transducers*, Coastal Engineering **11**, pp. 309 - 328 (1987). As referenced by Townsend, Murray and Fenton, John D., Numerical Comparisons of Wave Analysis Methods, *12th Australasian Coastal and Ocean Engineering Conference*, Melbourne, Institution of Engineers, Australia (May 1995).

5. Field, G., Knight, T., Mockford, T., & Nimmo, S., *Total Mine Simulation System Version 3.4.1 Volumes 1-4*, DRA TM (USM) 92129 - 92132, (1993)

6. Hamilton, L. J., *Bibliography of Wind-Wave Data and Publications for the Coastal Regions of Australia*, DSTO General Document DSTO-GD-0116 (1997).

7. Kulmar, M.A., Wave Direction Distributions off Sydney, New South Wales, *12th Australasian Coastal and Ocean Engineering Conference*, Melbourne, Institution of Engineers, Australia (May 1995).

8. Lawson and Treloar Pty Ltd., *Wave Modelling in Sydney Harbour*, DSTO Sydney Registry File 390-5-68(75), (14 December 1994).

9. Liu, Paul C., Normalized and Equilibrium Spectra of Wind Waves in Lake Michigan, *Journal of Physical Oceanography* **1**(4), 249-257, (1971).

10. Mitsuyasu, Hisashi, The One-Dimensional Wave Spectra at Limited Fetch, *Proceedings of the Thirteenth Coastal Engineering Conference, Vancouver, B.C.* , **1**, 289-306, ASCE (1972).

11. NSW Public Works, *Sydney Directional Waverider Buoy*, Manly Hydraulics Laboratory, Interim Report MHL656, (April 1995).

12. Saiva, G., *An Outline for the Analysis of Wave Induced Bottom Pressure Fluctuations*, MRL Technical Note MRL-TN-558, MRL, DSTO, (1989).

13. Saiva, Guntars, *An Exploratory Study of Surface Waves and the Corresponding Bottom Pressure Fluctuations*, MRL Technical Note MRL-TN-560, MRL, DSTO, (1989).

14. Wilson, J. R., *Referee Report on Draft Paper,* Australian Water and Coastal Studies Pty Ltd, (19 April 1996). DSTO Sydney Registry File 510-207-0558

7. Glossary

spectral width	a measure of the rms width of the wave energy density spectrum
Waverider	a floating buoy used to measure water level variations caused by ocean waves
zero crossing period	mean time interval between events at which the pressure or water level equals the mean level and is increasing

Appendix 1: Wave Modelling in Sydney Harbour

Reproduction of letter from Lawson and Treloar Pty Ltd to DSTO Sydney setting out details of the wave modelling performed under contract [8].

LAWSON AND TRELOAR PTY LTD
Coastal, Ocean and Water Resources Consulting Engineers

Directors
N.V. Lawson BE(Hons), MEngSc, CPEng
P.D. Treloar BE(Hons), ME, PhD, CPEng, MASCE
R.S. Carr BE(Hons), MSc, PhD, CPEng
A.D. McCowan BE(Hons), DipHE, PhD, CPEng, MASCE
R.A. Rice BE(Hons), BSc, MEngSc, CPEng

Unit 24, Norberry Terrace
177-199 Pacific Highway
PO Box 799,
North Sydney NSW 2060
Australia
Phone +61-2-922 2288
Fax +61-2-922 1195

14 December, 1994

Maritime Operations Division,
Aeronautical and Maritime Research Laboratory,
Defence Science and Technology Organisation,
Department of Defence,
P.O.Box 44,
PYRMONT NSW 2009

Your Ref: 390-5-68
Our Ref: L5651/J1275
Attn: Dr John Barnes

Dear Sirs,

RE: Wave Modelling in Sydney Harbour

We have completed the wave modelling of Sydney Harbour in terms of wave coefficients for your six directions and seven wave periods, namely:-

- south, south-south-east, south-east, east-south-east, east and north-east.
- 5, 8, 10, 12, 15, 19 and 50 seconds.

Wave coefficients at 47 locations to HMAS Penguin and Bradleys Head, as shown on Chart AUS 200, have been submitted to DSTO. Bathymetry was prepared from Charts AUS 200, 201 and 808. For wave periods other than 50 seconds, the Danish Hydraulic Institute model MIKE-21 Nearshore Waves (NSW) was used.

In the offshore region, rectangular grids of 50m in the direction of principal wave propagation by 250m in the orthogonal direction were prepared for each of the six dominant offshore wave directions. The model included directional spreading using the generalised cosine squared function, $\cos^n$, wherein n was set to be 40, equivalent to a standard deviation in directional spread of ~~18°~~ 9°. The outer grid models provided results for points 1 to 16. See letter from Doug 23/1/95

A fine grid model of Sydney Harbour was established in the east–west by north–south direction with a rectangular grid system of 20m (east–west) by 100m (north –south). Model output from each outer model run was transferred to the eastern boundary of the inner model to provide model input.

For the period of 50 seconds the reverse ray frequency–direction refraction/shoaling model RAYTRK was used with directional spreading the same as that used with the MIKE–21 NSW model. One model of the whole area was used with grid size varying from 100m to 400m.

Wave propagation to Bradleys Head is affected significantly by the Western Channel and Sow and Pigs formation with concentrations of wave energy from some offshore directions. Waves propagating in shallow water at small angles to dredged trenches may cause wave reflection and the Western Channel causes this phenomenon for the largest wave periods Generally, wave penetration reduces rapidly away from the main lead to Grotto Point as a result of refraction and sheltering. All model results are relative to a depth of 65m.

We have submitted the model results on DOS diskette, a copy of Chart AUS 200 and example plots under separate cover and hope that the work is completed to your satisfaction. Our final invoice is attached.

If you have any questions please do not hesitate to contact me.

Yours faithfully
LAWSON AND TRELOAR PTY LTD

P D TRELOAR

Appendix 2: Errors and Uncertainties

A2.1 Introduction

Mine actuation probability is largely a function of a weighted average of the components of the bottom pressure spectrum. Consequently, accurate predictions of mine actuation probability can be made in spite of large random errors in the individual components. Detailed investigation of the uncertainties in spectral estimates is necessary to try to improve the methods and to look for systematic errors affecting estimates of mine actuation probability.

Figure A2.1 shows the predicted and measured spectra for each of the 4 days and sites while Figure A2.2 shows their ratio. Most of the energy in each spectrum is concentrated in the range 0.05 to 0.15 Hz, and fortunately the agreement between the predicted and measured components is best at these frequencies, with median ratio near 1, and with most measurements lying within a factor of two of the median values. Outside this range, the errors increase. The uncertainties responsible for these errors are discussed below.

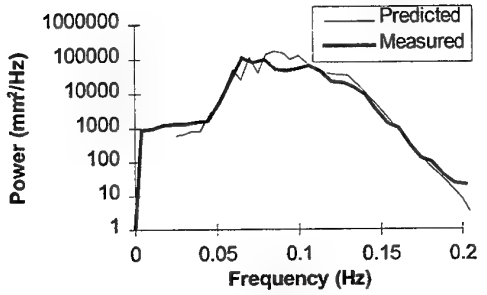

(a) 26 Oct Site 10

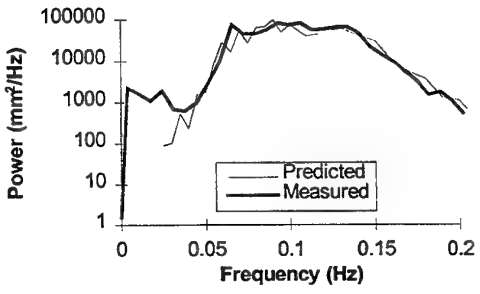

(b) 26 Oct Site 20

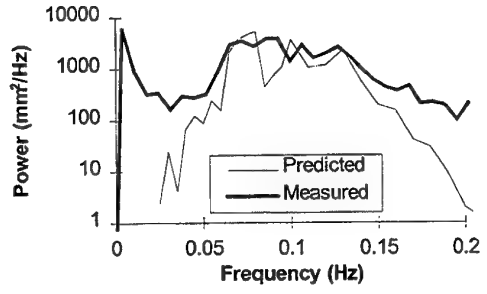

(c) 26 Oct Site 36

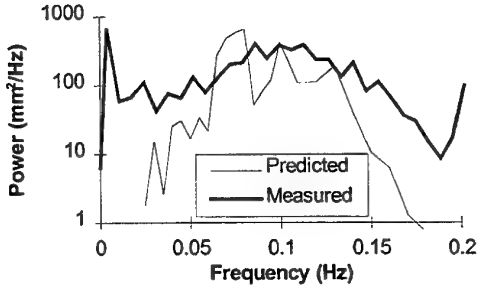

(d) 26 Oct Site 45

Figure A2.1 Comparison between Measured and Predicted Spectra (continued overleaf)

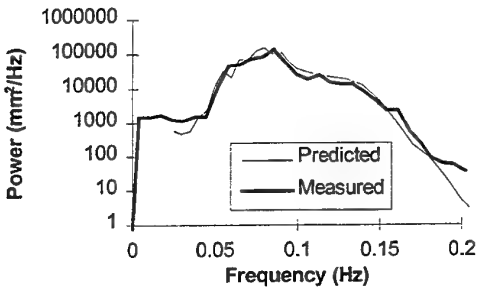

(e) 13 Sep Site 10

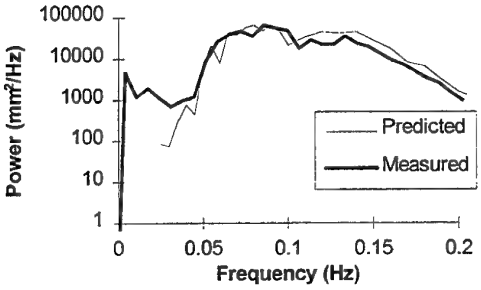

(f) 13 Sep Site 20

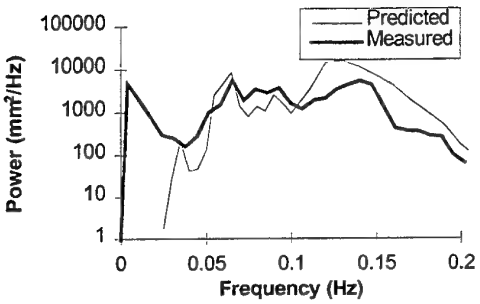

(g) 13 Sep Site 36

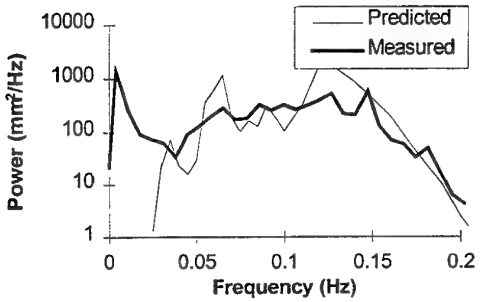

(h) 13 Sep Site 45

Not measured
(i) 4 July Site 10

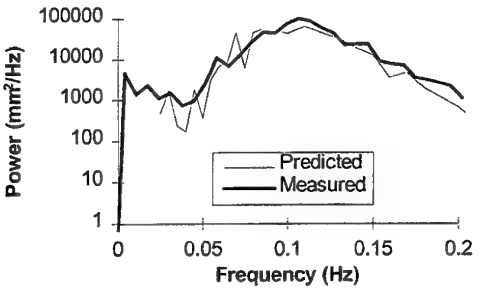

(j) 4 July Site 20

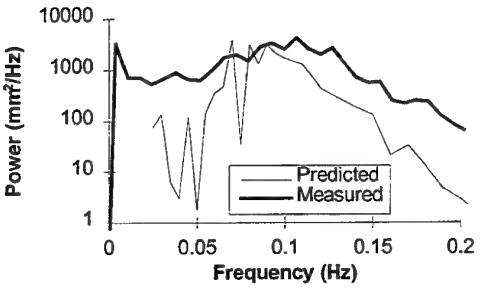

(k) 4 July Site 36

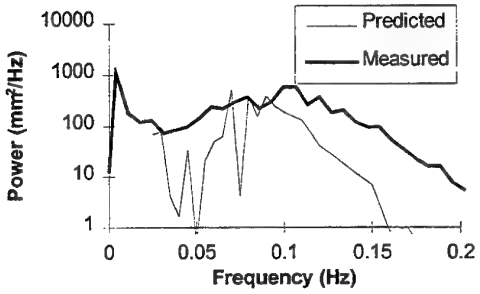

(l) 4 July Site 45

Figure A2.1 (cont.) Comparison between Measured and Predicted Spectra (continued overleaf)

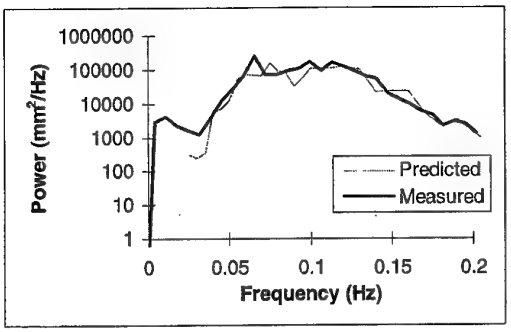

Not measured
(m) 6 June Site 10

(n) 6 June Site 20

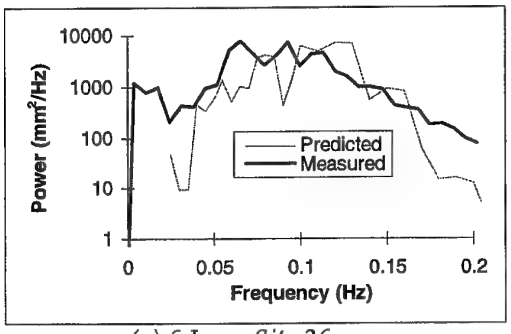

(o) 6 June Site 36

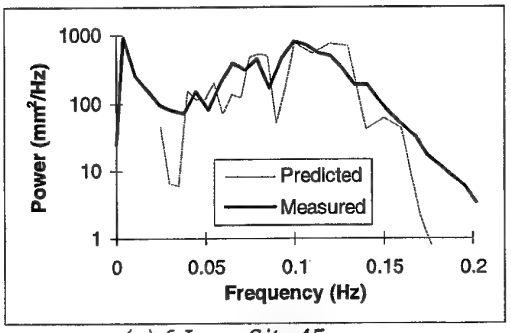

(p) 6 June Site 45

Figure A2.1 (cont.) Comparison between Measured and Predicted Spectra

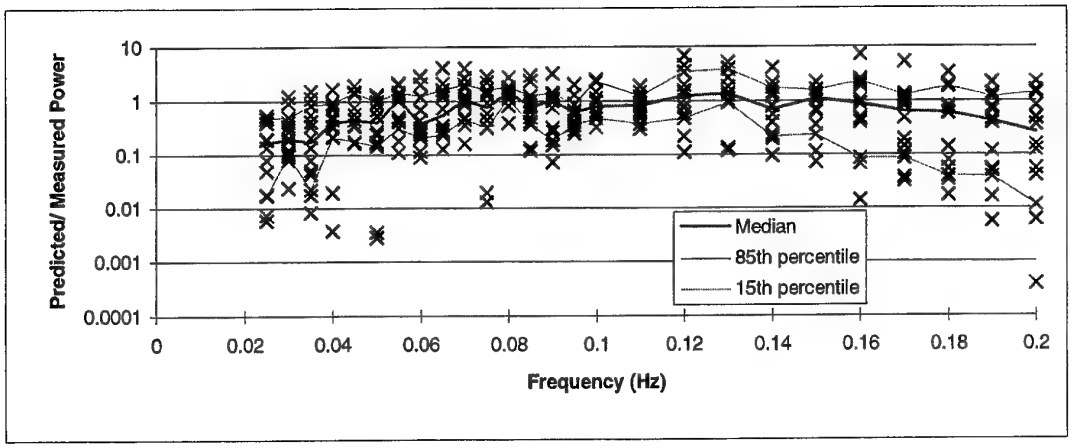

Figure A2.2 Accuracy of Predictions as a Function of Frequency
The graph shows the ratio of the predicted spectral power to the measured spectral power for each site and day as a function of the frequency. For a normal distribution, the 85th and 15th percentiles correspond to the mean plus or minus the standard deviation.

A2.2 Offshore Wave Spectra

Like all spectral measures, the offshore wave spectral estimates from the Waverider buoy are uncertain because of the finite sample time. An indication of the uncertainty in the spectral estimates can be seen in the differences between consecutive estimates (Fig. A2.3). Any trend is swamped by random fluctuations, which have a standard deviation equal to about 30% of the mean value. This explains much of the error between the measured and predicted spectra shown in Figure A2.2. Comparison of Figure A2.3 with Figure A2.1 also suggests the same conclusion.

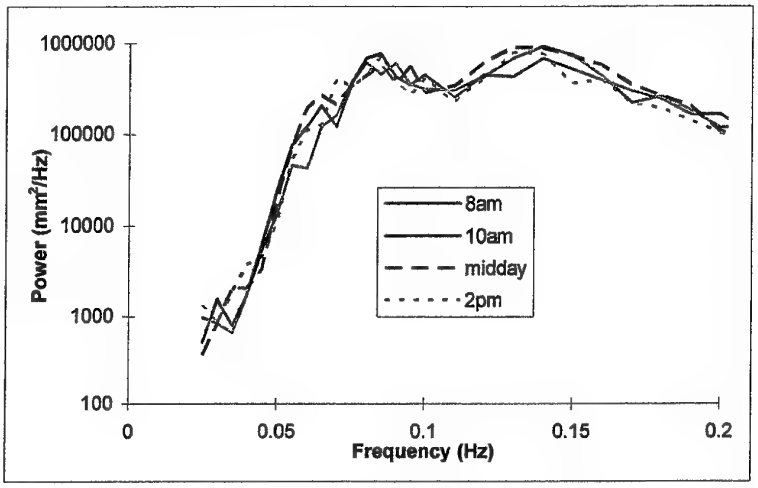

Figure A2.3 Variation of Consecutive Offshore Wave Spectral Power Estimates Spectra are for 13 September 1995

Improved agreement between predicted and measured spectra could theoretically be achieved by calculating the travel times for each spectral component to the measurement location, and using Waverider spectral estimates at different times equal to the measurement site time less the appropriate travel time, which varies by a few minutes with the spectral component velocity. However, variation with the spectral estimates is not practical given the standard Waverider output is two hourly.

Consecutive direction estimates from the Waverider buoy (Fig. A2.4) indicate a large uncertainty in the mean direction, particularly for the low frequencies (< 0.05 Hz). Because attenuation coefficients for the inshore sites are strongly dependent on wave direction, this uncertainty causes a large error in the low frequency components of the predicted bottom spectra. Figure A2.5(a) shows the uncertainty may reach a factor of 10 at low frequencies, and a factor of 2 at the main frequencies. This uncertainty is much greater than that caused by the offshore spectral magnitude uncertainty, (Fig. A2.5(b)). Although there is little background energy at low frequencies, much of the ship signature is at these frequencies [2], so filters in pressure mines will emphasise these frequencies, subject to the limitation of removing the very low frequency tidal components. The inability of the Waverider buoy to measure waves of frequency less

than 0.025 Hz may also be a major limitation, and is the subject of further study at DSTO.

The combined uncertainty in the bottom spectra predictions caused by the uncertainties in offshore spectral magnitudes and directions (Fig. A2.5(c)) explain the bulk of the differences between the measured and predicted spectra (Fig. A2.2).

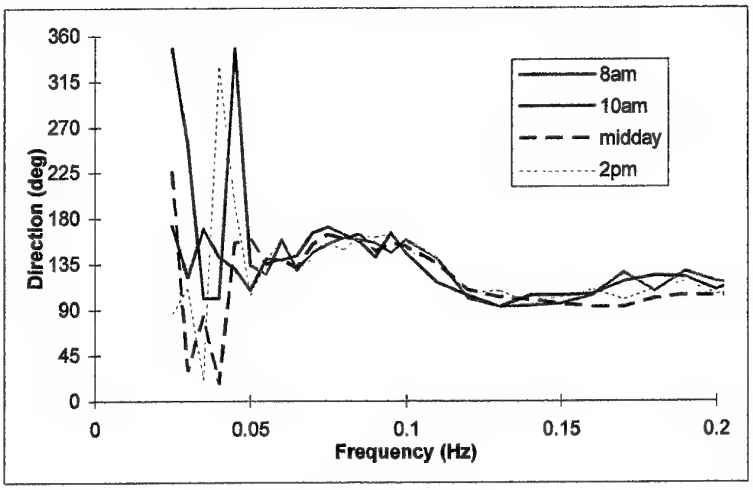

Figure A2.4 Variation of Consecutive Offshore Wave Spectra Mean Direction Estimates Spectra are for 13 September 1995

A2.3 Wave Refraction Attenuation Coefficients

Wave refraction was mainly studied using the Mike 21 NSW model (Danish Hydraulic Institute) by Lawson and Treloar Pty Ltd (Appendix 1). A bathymetric grid with spacing 50m by 250m (50m in the direction of principal wave propagation) was used offshore, and a finer grid of 20m by 100m used inshore. The model ignores diffraction. Although Mike 21 allows for non-linear effects, the techniques outlined in this report implicitly assume linear addition of the spectral components. For long period waves (50 seconds), a reverse ray model RAYTRK was used. The errors in the wave modelling are expected to be small compared to other errors *(P.D. Treloar, personal communication 12/12/95)*.

Wave refraction attenuation coefficients were only calculated for a small number of frequencies and mean offshore wave directions, with interpolation used to calculate the coefficients for intermediate frequencies and directions. The agreement between the measured and predicted spectra is not noticeably better for the calculated frequencies than the intermediate frequencies, suggesting that interpolation in the frequency domain is not a major source of error (Fig. A2.6). The strong dependence of refraction coefficient on direction suggests that interpolation for the appropriate direction could be a major source of error but again this is not confirmed by the measurements (Fig. A2.7). The reasons for this are discussed below.

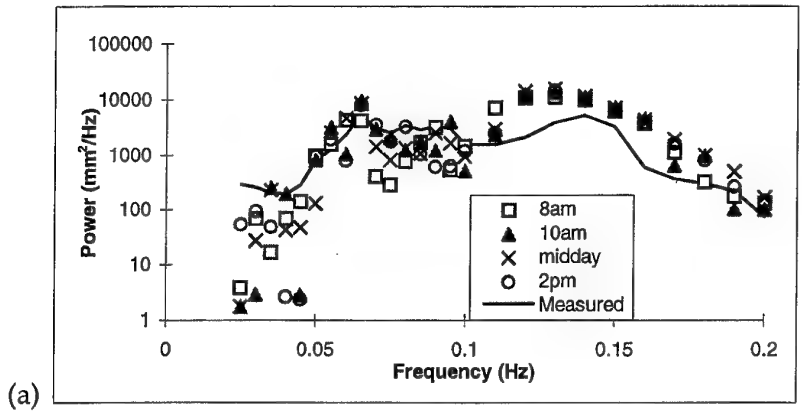

(a)

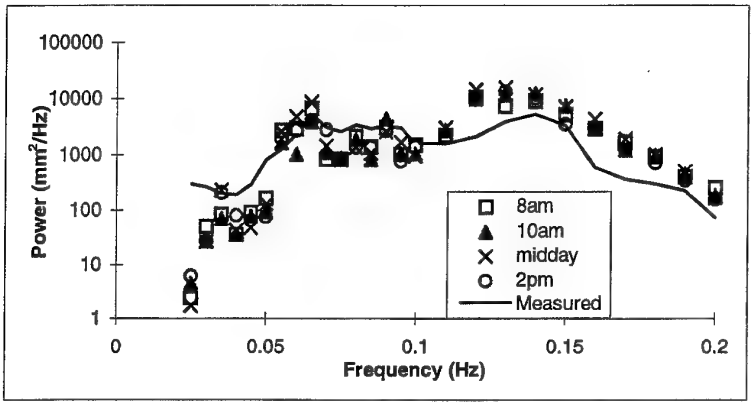

(b)

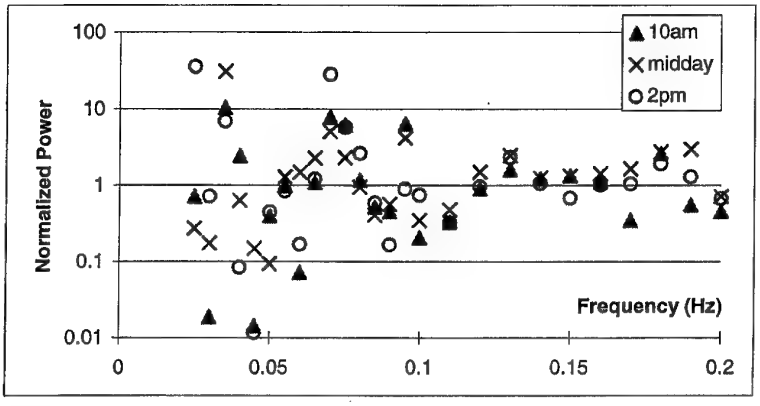

(c)

Figure A2.5 Variation of Predicted Bottom Spectra with Consecutive Offshore Spectral Estimates.
All spectra are for 13 September 1995, at site 36. Measurement at 12:30 pm. Predictions using consecutive estimates of:
(a) spectral directions, but constant magnitudes from midday spectrum;
(b) spectral magnitudes, but constant directions from midday spectrum;
(c) spectral magnitudes and directions. Each bottom spectral component is normalized relative to the corresponding component at 8am.

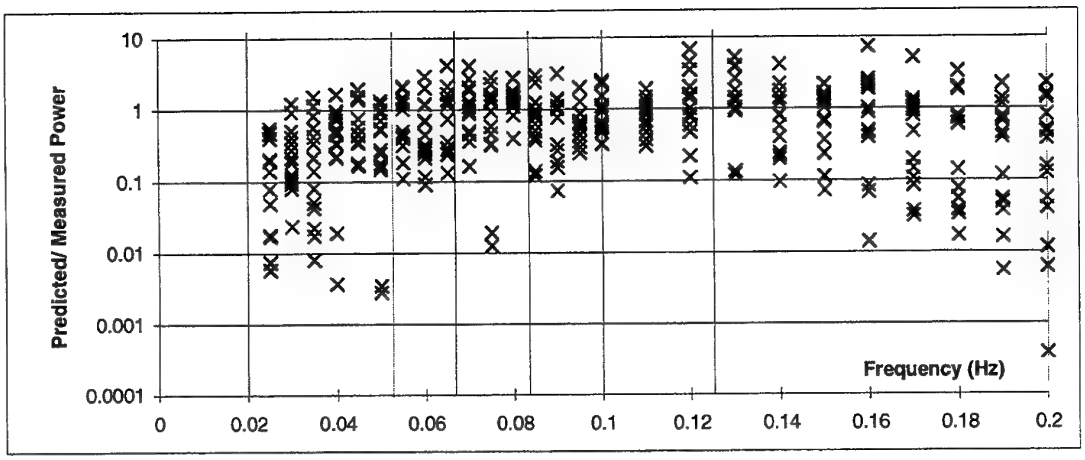

Figure A2.6 Accuracy of Predictions as a Function of Frequency
The graph shows the ratio of the predicted spectral power to the measured spectral power for each site and day as a function of the frequency. The vertical lines on the graph indicate the frequencies used in the refraction model, namely 0.020, 0.053, 0.067, 0.083, 0.100, 0.125 and 0.200 Hz, (periods of 50, 19, 15, 12, 10, 8 and 5 seconds).

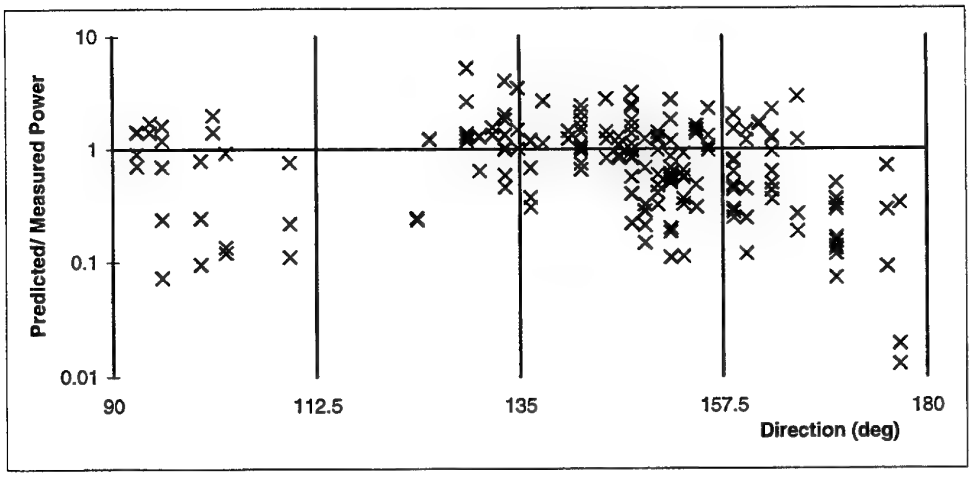

Figure A2.7 Accuracy of Predictions as a Function of Mean Direction
The graph shows the ratio of the predicted spectral power to the measured spectral power for each site, day and frequency bin as a function of the mean direction estimate. The frequency bins have been restricted to the frequencies 0.05 to 0.15 Hz where the offshore directional estimates are more certain (Fig. A2.4). The vertical lines on the graph indicate the directions used in the refraction model, namely 45°, 90°, 112.5°, 135°, 157.5° and 180°.

Wave refraction modelling was performed for each of the six specified directions assuming that for each frequency, the spectral density as a function of direction equals $\cos^{40}(\theta - \theta_m)$, where θ_m is the mean direction. This corresponds to a standard deviation of 9°. Lawson and Treloar claim that this is realistic for swell waves at Port Kembla (*personal communication 23/1/95*). However, for most frequencies, the measured directional spread from the Waverider buoy (which is approximately equal to the standard deviation) equals 40°, increasing to almost 90° at low frequencies (Fig. A2.8). Attenuation coefficients for a given mean direction used in this report were obtained by simply interpolating between the values calculated for the adjoining model frequencies. This corresponds to using the weighted average of two $\cos^{40}(\theta - \theta_m)$ distributions centred on the adjoining model frequencies. Figure A2.9 compares the typical direction spectrum used for the system output with a measured direction spectrum (the complete details of the actual direction spectrum are not known, and so a gaussian distribution is shown with the measured standard deviation). The figure suggests that it would be better in future to use a wider directional spread in the wave refraction models. Alternatively, a weighted average from more than two adjoining model frequencies could be used.

Given the large directional spread at low frequencies, together with the uncertainty in the mean direction at these frequencies, a better estimate of the bottom spectra may be calculated by assuming a uniform distribution of wave energy from all seaward directions, rather than a narrow distribution at the estimated mean direction. Taking as an approximation to this a mean direction of 135°, the estimates are greatly improved at low frequencies (Fig. A2.10).

Because the directional spread of the measured spectrum is generally sufficiently wide to encompass a few of the modelled spectra, it is not surprising that the system accuracy is similar regardless of whether the mean direction lies at or half way between the modelled mean directions (Fig. A2.7).

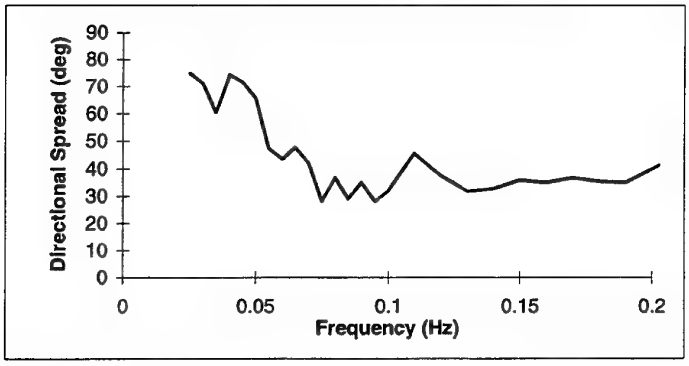

Figure A2.8 Typical Directional Spread for Each Frequency Bin Midday, 13 September 1995

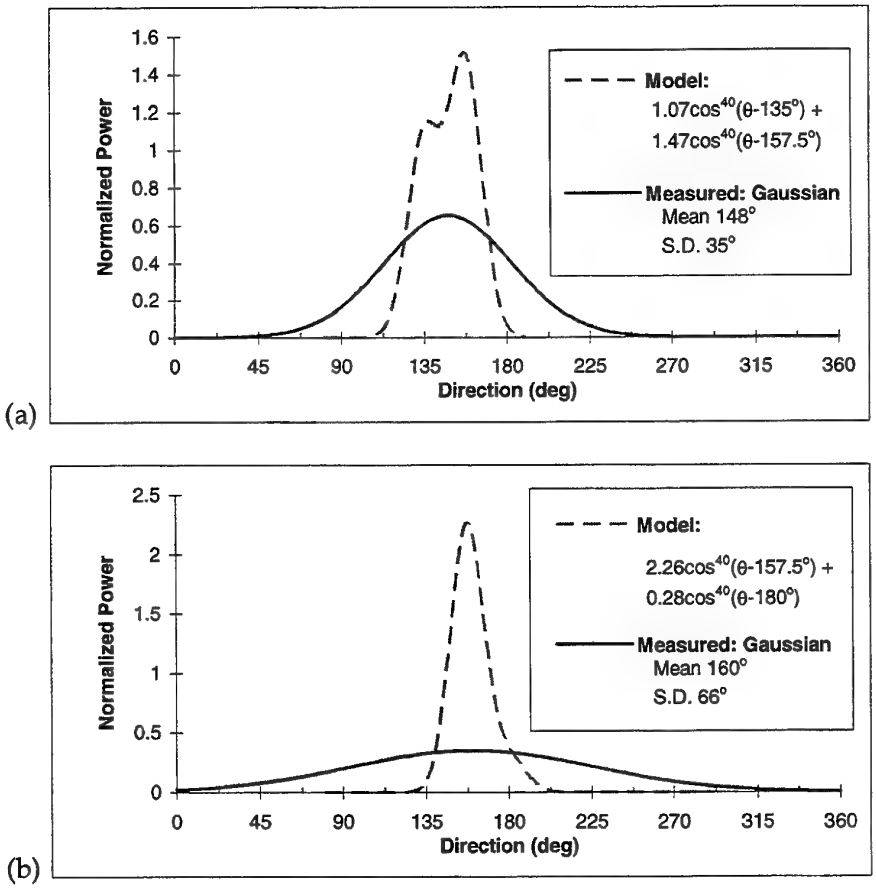

Figure A2.9 Model and Actual Directional Spectra
(a) Frequency bin centred on 0.09Hz, midday, 13 September 1995.
(b) Frequency bin centred on 0.05Hz, midday, 13 September 1995.

A2.4 Local Generation of Waves

Waves can be generated within harbours by the action of the local wind. Because the fetch (length of water over which the wind blows) is generally small, the waves are generally small and short (high frequency), and so are strongly attenuated with depth. Any effects from locally generated waves will be most noticeable at shallow sites most protected from the offshore swell i.e. furthest up the harbour.

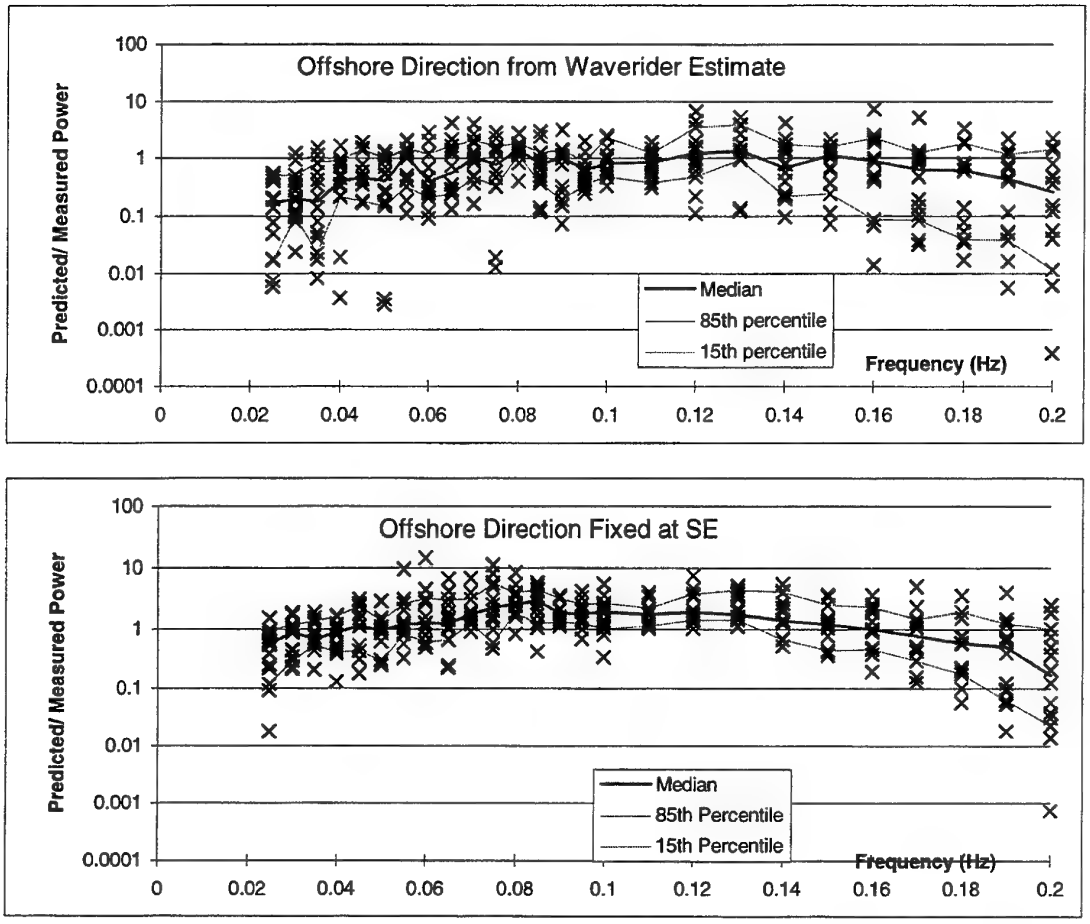

Figure A2.10 Comparison of Accuracy of Predictions as a Function of Frequency using Waverider Direction Estimate or Fixed SE Direction

For site 45, the fetch is always less than 6 km, and the wind speed is generally less than 10m/s. Using these values, and applying Liu's spectrum [9], the peak spectral component in the bottom spectrum (25m depth) is only 7 mm^2/Hz at 0.21 Hz (Fig. A2.11). This is negligible compared to the peak measured spectral component of 500-1000 mm^2/Hz at 0.1 to 0.15 Hz. However, at 0.2 Hz and above, locally generated waves may be a major source of energy for site 45, but only if the winds are both strong and from the NE quadrant, a combination which did not occur during our measurements. There is some uncertainty in the theoretical prediction, as it is mainly designed to accurately predict the spectra at frequencies near the peak frequency at the surface, and not at the lower peak frequency at the sea bed. Using Mitsuyasu's formula II [10], the energy is an order of magnitude less.

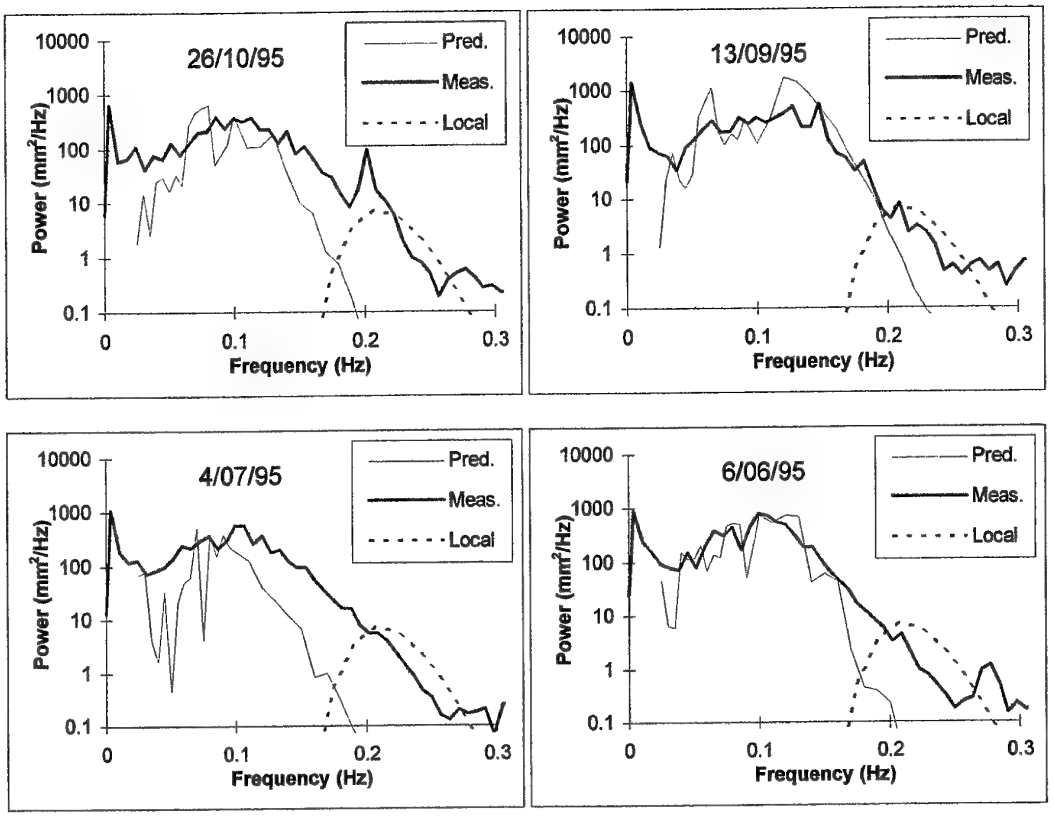

Figure A2.11 Comparison of Measured Spectra with Waverider Prediction and Possible Local Generation for Site 45
Local generation is based on a 10m/s wind acting over a 6 km fetch according to the theory of Liu [9].

Waves within harbours can also be generated by shipping, particularly ferries and other small craft. Figure A2.12 shows the power spectra generated by shipping at the seabed below the Sydney Harbour Bridge [2]. This location is well protected from offshore swell. At 3 am, when shipping is minimal and winds are low, there is little wave activity, apart from the tidal fluctuations. At midday, the power is greatly increased, because of the waves generated by ferries and other small craft. The spectra are calculated from a 34 minute record, so no significant difference is seen on those occasions when there was a single large merchant ship transit. Spectra recorded at 8 am, when the winds are light but ferry traffic is similar to midday, are similar to those at midday, confirming that it is the shipping traffic and not the local winds generating the waves.

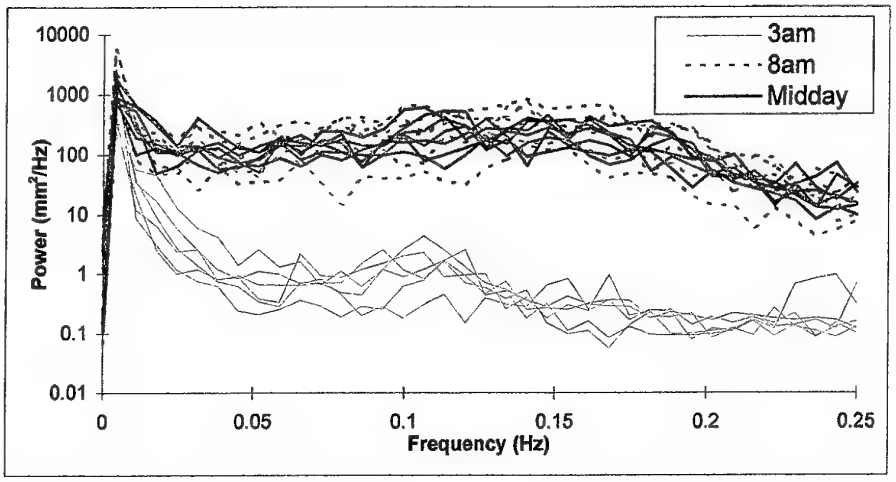

Figure A2.12 Bottom spectra recorded below the Sydney Harbour Bridge in approximately 15m depth of water [2]. Spectra are shown for several days at 3 am, 8 am and midday.

Figure A2.13 shows the spectra calculated from bottom pressure measurements at sites 36 and 45, compared to that calculated from measurements below the Sydney Harbour Bridge at midday. At 0.1 Hz, there is a large power component due to swell seen at site 36, and to a lesser extent at site 45. At 0.15 to 0.25 Hz, the swell component is reduced, and the power at both sites 36 and 45 drops to levels similar to those below the bridge, (allowing for the different depths), and is attributed to background shipping. It is reasonable that background shipping will cause similar wave activity at sites 36, 45 and below the bridge, as both sites 36 and 45 are on the Circular Quay to Manly ferry route, while there are several ferry routes passing below the bridge. For site 45, background shipping also appears to dominate at low frequencies (<0.05 Hz).

It must be stressed that the average contribution from background shipping to the bottom pressure spectrum is small, and is only seen at sheltered locations at frequencies where the energy is small relative to the spectral peak.

A2.5 Attenuation with Depth

Saiva [13] summarizes research suggesting that the use of linear wave theory to predict attenuation of pressure fluctuations with depth overestimates the bottom spectra by up to 100%. The greatest overestimate is expected at low frequencies. No evidence of this systematic error can be seen in the data collected in this experiment (Fig. A2.2), suggesting that it is not a major error. Bishop and Donelan [4] and Wilson [14] also suggest that the errors due to calculation of attenuation with depth are small. Figure A2.14 shows that no supporting evidence is forthcoming even for site 10, the furthest offshore of the measurement sites, where the errors associated with wave refraction are likely to be minimized, and the depth is greatest.

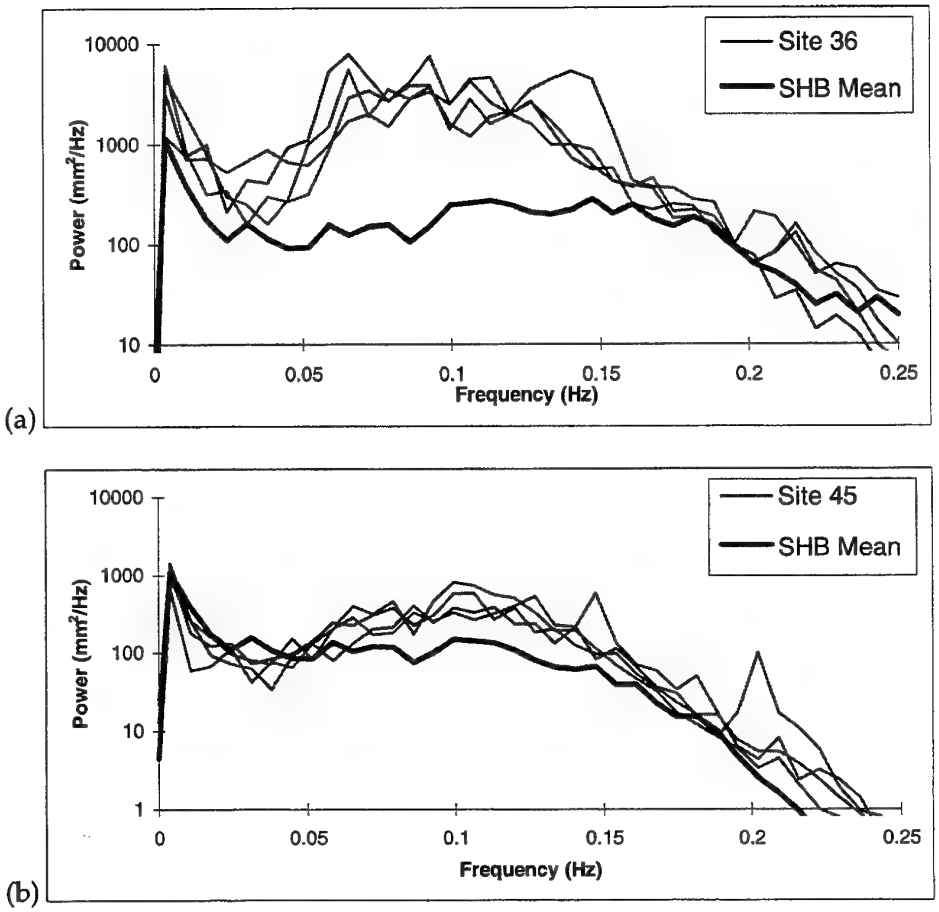

Figure A2.13 Measured Bottom Pressure Spectra at Site 36, Site 45 and below the Sydney Harbour Bridge.
(a) Bottom pressure spectra at site 36 and below the bridge.
(b) Bottom pressure spectra at site 45 and below the bridge. The Sydney Harbour Bridge spectral components have been attenuated in (b) to match the 25m depth at site 45, rather than the depth at the bridge site of 15m.

A2.6 Bottom Pressure Measurements

Similar large uncertainties in the measured bottom pressure spectral estimates are caused by the finite sampling period as occur with the offshore spectral magnitude estimates. These ultimately limit the accuracy of direct measurements of bottom spectra and mine actuation probability as an alternative to the prediction techniques presented in this report.

Errors in spectral estimates made from direct measurements of bottom pressure fluctuations also cause errors in the estimates of mean amplitude, zero crossing period Tz and spectral width υ. The magnitude of these errors is not easily calculated theoretically, but the standard deviation is approximately equal to the root mean square difference between consecutive estimates divided by $\sqrt{2}$, assuming that the rate of change of the parameters is comparatively small. While long term measurements have not been made at the sites in Sydney Harbour, Table A2.1 indicates the standard deviation of consecutive bottom pressure measurements at other locations. The standard deviation of the amplitude, Tz and υ measurements is of order 9%, 3% and 13% respectively, but is strongly dependent on the site.

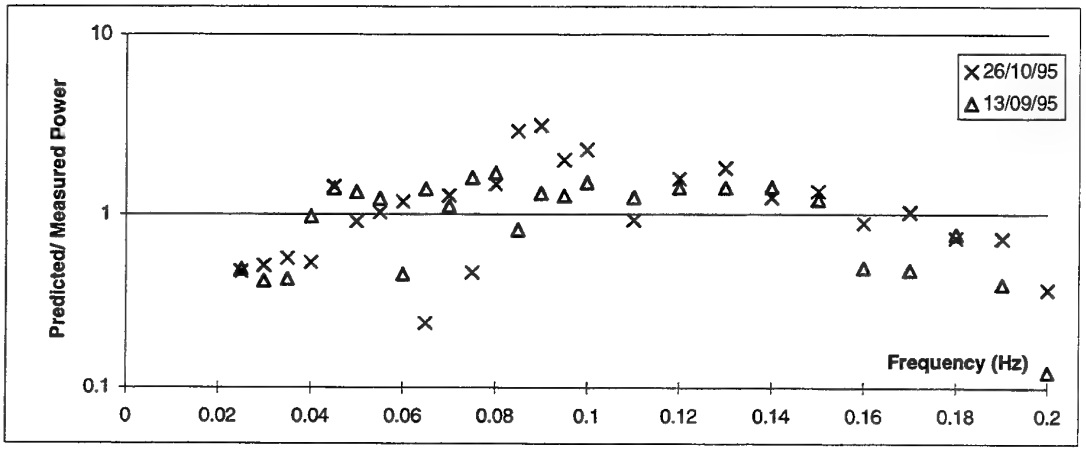

Figure A2.14 Accuracy of Predictions as a Function of Frequency for Site 10

Table A2.1 Variability of Consecutive Direct Bottom Pressure Measurements
The standard deviation of the parameters is taken as the root mean square difference between consecutive measurements divided by $\sqrt{2}$.

Trial Location	Interval (hours)	Depth (m)	Amplitude (mm)		Tz (sec)		υ	
			Mean	S.D.	Mean	S.D.	Mean	S.D.
Hunters Bay	3	10	101	11 (11%)	10.2	0.3 (3%)	0.33	0.02 (6%)
Jervis Bay	1	18	23	2 (8%)	9.9	0.4 (4%)	0.42	0.08 (19%)
Townsville Offshore	1	18	53	3 (7%)	7.0	0.1 (2%)	0.19	0.03 (15%)
Average	2	15	59	5 (9%)	9.0	0.3 (3%)	0.31	0.04 (13%)

To avoid obstruction to shipping, and reduce contamination of the environmental pressure measurements by ship signatures, measurements were not made precisely at the sites shown in Figure 3, but occurred up to 300m away. As the techniques

developed in this report were developed in response to spatial variations in actuation probability and bottom pressure spectra along the shipping routes, this is an important error to analyse. Spatial variations are caused by changes in both the wave refraction attenuation coefficients and the depth attenuation coefficients. No error between predictions and measurements will result from the latter because the predictions were calculated using the depth recorded during the pressure measurements. An indication of the errors associated with the former can be seen by the change in wave refraction attenuation coefficient between adjacent sites (spacing 250m), which is generally less than about 30% (Fig. A2.15).

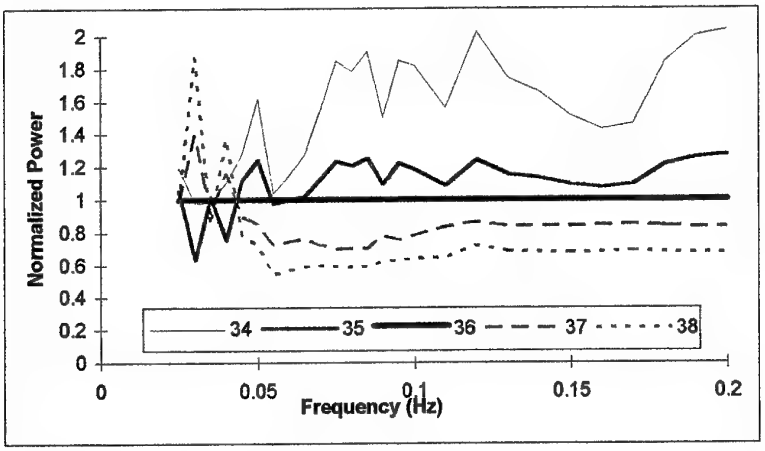

Figure A2.15 Variation in Spectra Caused by Change in Wave Refraction Attenuation Coefficients between Adjacent Sites
The spectra have been calculated assuming a uniform depth of 15.7m, and using the offshore spectral file for midday on 13 September 1995 for the appropriate directions.

A2.7 Summary of Uncertainties

The techniques outlined in this report do not produce vastly greater uncertainties at the dominant frequencies than those associated with direct measurement of bottom spectra. The uncertainties were shown in the body of the report to be sufficiently small to allow accurate prediction of mine actuation probability.

The major uncertainties are summarized in Table A2.2. Most of the energy in the bottom spectra is concentrated in the frequency range 0.05 to 0.2 Hz, and at these frequencies uncertainties in the spectral estimates from the Waverider buoy and the bottom pressure measurements are significant uncertainties which each explain a large part of the differences between measurements and predictions.

At low frequencies, uncertainties in the directional estimates and errors in the directional modelling produce uncertainties equal to an order of magnitude. While the energy at these frequencies is less than in the main frequency range discussed above,

pressure mines may be designed to focus on these frequencies because of the ship signature energy at these frequencies. Better modelling techniques should reduce these errors.

Waves generated by ferries and other small craft produce a small amount of background energy. This is significant for sheltered locations at the higher frequencies.

Further investigations of the major uncertainties, and methods to reduce them, are continuing. Better matching of the modelled directional spread with measurements is being investigated. Offshore spectral uncertainties are being compared with theoretical predictions and other measurements. Better spectral estimates might be obtained by averaging consecutive spectra, depending on the rate at which the true spectrum changes with time. Low frequency direction estimates might be improved by smoothing over adjacent frequency bins.

Table A2.2 Summary of Uncertainties
Low frequencies are those less than 0.05 Hz, while the main frequencies in the bottom spectrum are from 0.05 to 0.2 Hz. The size of the uncertainty is the uncertainty caused in the bottom spectral estimates.

Cause	Size of Uncertainty
Offshore Spectral Estimates	
Magnitude Estimates	30%
Direction Estimates	Factor of 10 at low frequency, and 2 at main frequencies
Wave Refraction Model	
Model Results	Relatively Small
Interpolation of Frequencies	Relatively Small
Interpolation of Directions	Relatively Small
Directional Spread	Factor of 10 at low frequency coupled with uncertainty in direction estimate
Local Generation of Waves	
Wind generation of waves	Negligible for frequencies less than 0.15 Hz. Possibly significant at higher frequencies for high winds not observed during trial.
Background Shipping	Dominant in locations more sheltered from swell, at frequencies greater than 0.15 Hz.
Depth Attenuation	100%?
Bottom Pressure Measurements	
Spectral Estimates	30%
Position Offset	30%

Appendix 3: Non-Directional versus Directional Waverider Data

At many locations around Australia, the full offshore directional wave spectrum is not available [6]. In many cases, a single direction is given for the complete spectrum, based on visual observation, coupled with the magnitude spectrum from a non-directional Waverider. The effect on the accuracy of inshore spectral predictions caused by using this limited data is studied in this appendix. In line with the procedures used by Manly Hydraulics Laboratory, the single direction chosen is the direction at the peak spectral bin from the directional Waverider.

Figure A3.1 shows the ratio of the predicted to measured spectral components using the complete directional spectra and a single direction only. The accuracy appears to be moderately degraded with the single direction. Figure A3.2 also suggests this, showing an increased scatter in the plots of measured and predicted mean amplitudes, with the correlation dropping from 0.96 to 0.85. The rms difference between the measured and predicted zero crossing periods is constant at 0.9 seconds, while the rms error in the spectral width is constant at 0.35. However, the results with the single direction still provide a useful estimate in the absence of better predictions.

At low frequencies, the spectral estimates appear slightly better with the single direction than with the complete directional spectra. This is because, (as explained more fully in Appendix 2), a direction which is near the average of all waves propagating shorewards gives a better estimate of the average refraction attenuation coefficient for the wide directional spread at low frequencies than an estimate based on a narrow spectrum centred on the highly variable mean direction of individual spectral components. With the improvements to the techniques suggested in Appendix 2, it is expected that the results will be better with the complete directional spectrum for all frequencies.

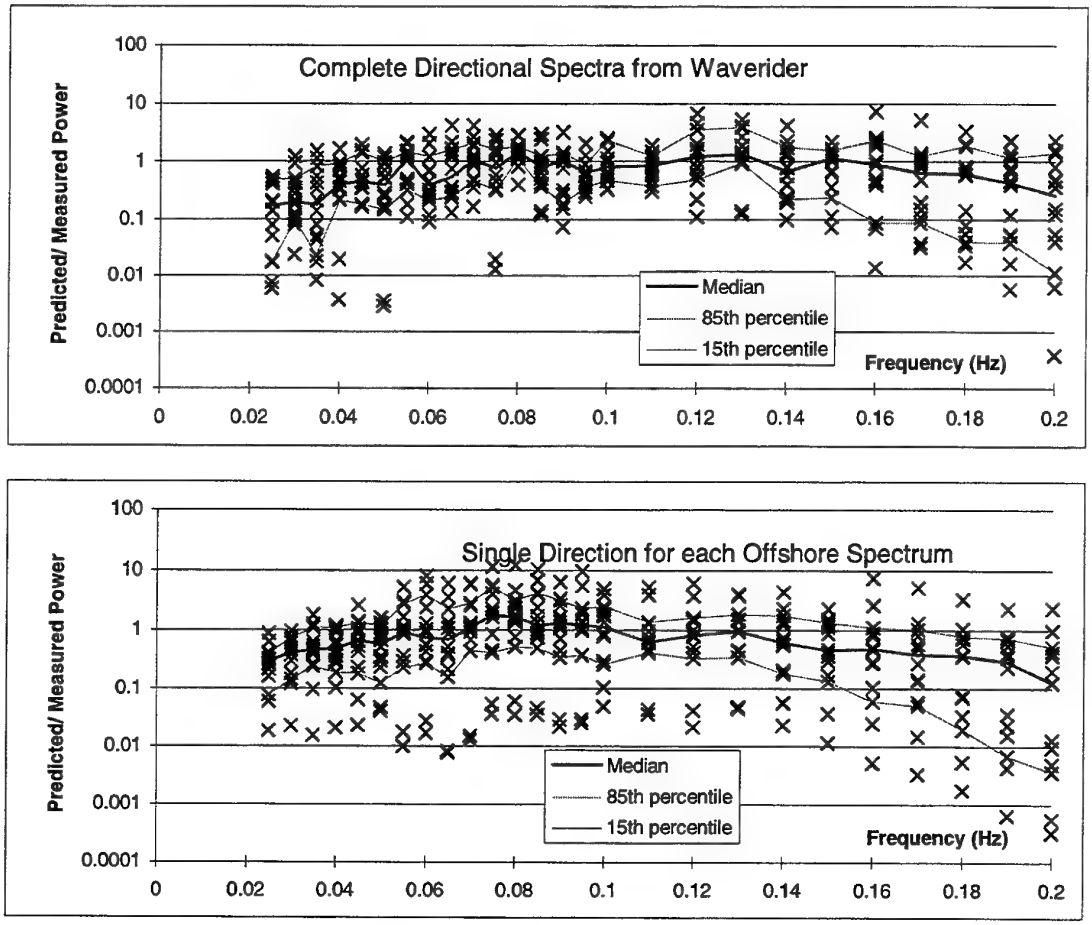

Figure A3.1 Ratio of the Predicted to Measured Spectral Components using the Complete Directional Spectra and a Single Direction Only
The single direction chosen is the direction at the peak spectral bin from the directional Waverider.

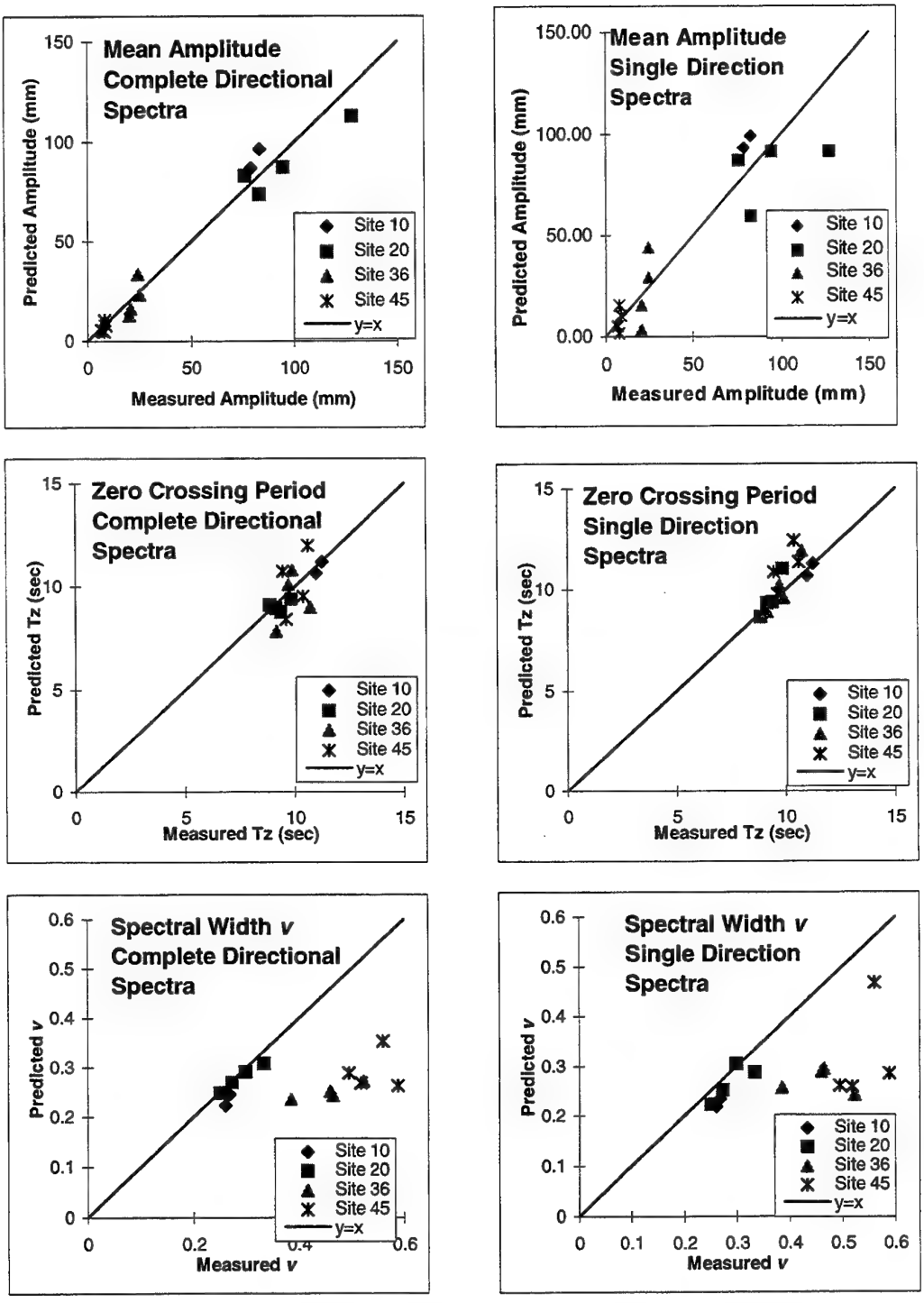

Figure A3.2 Predicted and Measured Significant Wave Mean Amplitudes, Zero Crossing Periods and Spectral Widths using the Complete Directional Spectra and a Single Direction Only

DISTRIBUTION LIST

New Techniques to Predict Ship Vulnerability to Pressure Mines along Shipping Routes

John C. Barnes

AUSTRALIA

DEFENCE ORGANISATION

Task Sponsor Director General Maritime Development

S&T Program

Chief Defence Scientist
FAS Science Policy
AS Science Corporate Management
} shared copy

Director General Science Policy Development
Counsellor Defence Science, London (Doc Data Sheet)
Counsellor Defence Science, Washington (Doc Data Sheet)
Scientific Adviser to MRDC Thailand (Doc Data Sheet)
Director General Scientific Advisers and Trials/Scientific Adviser Policy and Command (shared copy)
Navy Scientific Adviser
Scientific Adviser - Army (Doc Data Sheet and distribution list only)
Air Force Scientific Adviser
Director Trials

Aeronautical and Maritime Research Laboratory

Director
Chief of Maritime Operations Division
Dr Alan Theobald, MOD Sydney
Dr Bryan Jessup, MOD Sydney
Dr John Barnes, MOD Sydney
Mr Les Hamilton, MOD Sydney
Mr Angus MacInnes, MOD Sydney
Dr Don Richardson, MOD Melbourne
Mr Frank May, MOD Melbourne
Mr Robert Dow, MOD Melbourne
Dr Stephen Bocquet, AOD Melbourne
Mr David Cox, AOD Melbourne

DSTO Library

Library Fishermens Bend
Library Maribyrnong
Library Salisbury (2 copies)
Australian Archives
Library, MOD, Pyrmont
Library, MOD, HMAS Stirling

Capability Development Division

Director General Land Development (Doc Data Sheet only)
Director General C3I Development (Doc Data Sheet only)

Navy

Mine Warfare Systems Centre Project Director
COMAUSMINDIVFOR, HMAS Waterhen
Maritime Headquarters, DNW (Attention: SOMCD)
Hydrographer
Mine Hunter Coastal Project Director
OIC, Royal Australian Navy Ranges and Assessing Unit
OIC Mine Warfare School
OIC Mine Warfare Diving School
SO (Science), Director of Naval Warfare, Maritime Headquarters Annex, Garden Island, NSW 2000 (Doc Data Sheet and distribution list only)

Army

ABCA Office, G-1-34, Russell Offices, Canberra (4 copies)
SO (Science), DJFHQ(L), MILPO Enoggera, Queensland 4051 (Doc Data Sheet only)
NAPOC QWG Engineer NBCD c/- DENGRS-A, HQ Engineer Centre Liverpool Military Area, NSW 2174 (Doc Data Sheet only)

Intelligence Program

DGSTA Defence Intelligence Organisation

Corporate Support Program (libraries)

OIC TRS, Defence Regional Library, Canberra
Officer in Charge, Document Exchange Centre (DEC), 1 copy
*US Defence Technical Information Center, 2 copies
*UK Defence Research Information Centre, 2 copies
*Canada Defence Scientific Information Service, 1 copy
*NZ Defence Information Centre, 1 copy
National Library of Australia, 1 copy

UNIVERSITIES AND COLLEGES

Australian Defence Force Academy
Library
Head of Aerospace and Mechanical Engineering
Deakin University, Serials Section (M list), Deakin University Library, Geelong, 3217
Senior Librarian, Hargrave Library, Monash University
Librarian, Flinders University

OTHER ORGANISATIONS

NASA (Canberra)
AGPS

Dr P. D. Treloar
Lawson and Treloar Pty Ltd
PO Box 852
Pymble NSW 2073

Mr M. A. Kulmar
Manly Hydraulics Laboratory
110B King St
Manly Vale NSW 2093

Mr A. F. Nielsen
Australian Water and Coastal Studies Pty Ltd
110 King St
Manly Vale NSW 2093

Mr M. Willoughby
Sydney Ports Corporation
PO Box 25
Millers Point NSW 2000

Mr S. Buchan
WNI Science and Engineering
31 Bishop St
Jolimont W.A. 6014

OUTSIDE AUSTRALIA

TTCP Group G13 New Zealand National Leader
Mr I. Rumball
Defence Science Establishment
Private Bag 32901
Auckland Naval Base
Auckland, New Zealand

TTCP Group G13 United Kingdom National Leader
Mr John Wickenden
DRA Bincleaves
Newtons Rd
Weymouth, Dorset DT4 8UR, UK

TTCP Group G13 United States National Leader
Dr Wally Ching
Office of Naval Research
800 N. Quincy St
Arlington VA 22217-5660, USA

ABSTRACTING AND INFORMATION ORGANISATIONS

INSPEC: Acquisitions Section Institution of Electrical Engineers
Library, Chemical Abstracts Reference Service
Engineering Societies Library, US
Materials Information, Cambridge Scientific Abstracts, US
Documents Librarian, The Center for Research Libraries, US

INFORMATION EXCHANGE AGREEMENT PARTNERS

Acquisitions Unit, Science Reference and Information Service, UK
Library - Exchange Desk, National Institute of Standards and Technology, US

SPARES (10 copies)

Total number of copies: 81

DEFENCE SCIENCE AND TECHNOLOGY ORGANISATION
DOCUMENT CONTROL DATA

1. PRIVACY MARKING/CAVEAT (OF DOCUMENT)

2. TITLE

New Techniques to Predict Ship Vulnerability to Pressure Mines along Shipping Routes

3. SECURITY CLASSIFICATION (FOR UNCLASSIFIED REPORTS THAT ARE LIMITED RELEASE USE (L) NEXT TO DOCUMENT CLASSIFICATION)

Document	(U)
Title	(U)
Abstract	(U)

4. AUTHOR(S)

John C. Barnes

5. CORPORATE AUTHOR

Aeronautical and Maritime Research Laboratory
PO Box 4331
Melbourne Vic 3001 Australia

6a. DSTO NUMBER	6b. AR NUMBER	6c. TYPE OF REPORT	7. DOCUMENT DATE
DSTO-RR-0126	AR-010-458	Research Report	February 1998

8. FILE NUMBER	9. TASK NUMBER	10. TASK SPONSOR	11. NO. OF PAGES	12. NO. OF REFERENCES
510/207/0558	ADS 93/230	DGMD	37	14

13. DOWNGRADING/DELIMITING INSTRUCTIONS

None

14. RELEASE AUTHORITY

Chief, Maritime Operations Division

15. SECONDARY RELEASE STATEMENT OF THIS DOCUMENT

Approved for public release

OVERSEAS ENQUIRIES OUTSIDE STATED LIMITATIONS SHOULD BE REFERRED THROUGH DOCUMENT EXCHANGE CENTRE, DIS NETWORK OFFICE, DEPT OF DEFENCE, CAMPBELL PARK OFFICES, CANBERRA ACT 2600

16. DELIBERATE ANNOUNCEMENT

No Limitations

17. CASUAL ANNOUNCEMENT Yes

18. DEFTEST DESCRIPTORS

pressure minesweeping, pressure sweeps, pressure signatures, ocean waves, oceanographic data processing

19. ABSTRACT

New techniques have been developed which allow for real time prediction of ship vulnerability to pressure mines at all points along the shipping routes approaching and within Australia's priority ports. Rather than performing an extensive series of measurements, environmental bottom pressure fluctuations can be predicted using data from existing offshore wave measuring systems. The techniques have been validated by measurements in Sydney Harbour. In addition, sweep effectiveness can be predicted in real time, and seasonal averages of ship vulnerability and sweep effectiveness calculated for planning purposes.